Steady-State and Closed-State Inactivation Properties of Inactivating BK Channels

Jiu Ping Ding and Christopher J. Lingle

Washington University School of Medicine, Department of Anesthesiology, St. Louis, Missouri 63110 USA

ABSTRACT Calcium-dependent potassium (BK-type) Ca^{2+} and voltage-dependent K^+ channels in chromaffin cells exhibit an inactivation that probably arises from coassembly of *Slo1* α subunits with auxiliary β subunits. One goal of this work was to determine whether the Ca^{2+} dependence of inactivation arises from any mechanism other than coupling of inactivation to the Ca^{2+} dependence of activation. Steady-state inactivation and the onset of inactivation were studied in inside-out patches and whole-cell recordings from rat adrenal chromaffin cells with parallel experiments on inactivating BK channels resulting from cloned $\alpha + \beta 2$ subunits. In both cases, steady-state inactivation was shifted to more negative potentials by increases in submembrane [Ca^{2+}] from 1 to 60 μM. At 10 and 60 μM Ca^{2+}, the maximal channel availability at negative potentials was similar despite a shift in the voltage of half availability, suggesting there is no strictly Ca^{2+}-dependent inactivation. In contrast, in the absence of Ca^{2+}, depolarization to potentials positive to +20 mV induces channel inactivation. Thus, voltage-dependent, but not solely Ca^{2+}-dependent, kinetic steps are required for inactivation to occur. Finally, under some conditions, BK channels are shown to inactivate as readily from closed states as from open states, indicative that a key conformational change required for inactivation precedes channel opening.

INTRODUCTION

Inactivation of voltage-dependent channels often exhibits an apparent voltage dependence because of coupling of a voltage-independent or weakly voltage-dependent inactivation process to stronger voltage-dependent channel activation. Inactivation of a novel form of calcium (Ca^{2+})- and voltage-dependent K^+ channel, termed a BK_i channel (Solaro et al., 1995), found in most rat adrenal chromaffin cells and also pancreatic beta cells (Lingle et al., 1996; Li et al., 1999) also exhibits some dependence not only on voltage but also on [Ca^{2+}]. These properties are also shared with inactivating BK currents that arise from heterologous expression of the *Slo1* pore-forming α subunit (Adelman et al., 1992; Butler et al., 1993) with the $\beta 2$ auxiliary subunit (Wallner et al., 1999; Xia et al., 1999). For both the native BK_i channels and the cloned inactivating BK channels, this dependence has been proposed to arise from coupling of inactivation to both the Ca^{2+} and voltage-dependent transitions involved in BK channel activation. In general, such coupling is often assumed to arise specifically as a result of inactivation occurring from channel open states.

For BK channels, activation is governed by both Ca^{2+} and voltage-dependent transitions that precede channel opening (Wei et al., 1994; Cox et al., 1997; Horrigan et al., 1999; Horrigan and Aldrich, 1999; Rothberg and Magleby, 2000). Specifically, the most complete analysis of BK channel gating now suggests that four independent Ca^{2+}-binding steps and the independent movement of four voltage sensors allosterically participate in BK activation (Cox and Aldrich, 2000; Cui and Aldrich, 2000). Ca^{2+} binding and voltage-sensor movement appear to be largely independent processes, although there has been a suggestion that, in the presence of the $\beta 3$ auxiliary subunit, there may be voltage-dependent transitions that influence Ca^{2+} binding affinity (Zeng et al., 2001). In light of current thinking about BK channel gating, it is therefore worthwhile to consider whether inactivation may be specifically coupled to Ca^{2+} binding steps, to movement of voltage-sensors, or to channel opening per se. Thus, one aim of the present work was to further define properties of inactivation of BK channels that might be informative about the types of transitions that are necessary for inactivation to occur.

The work described here also addresses two other aims. First, because of the possibility that the availability of native BK_i channels in native cells may undergo dynamic regulation under normal chromaffin cell activity as a consequence of inactivation (Herrington et al., 1995), we examine properties of BK current inactivation at [Ca^{2+}] and membrane potentials that are likely to occur during normal physiological activity. In earlier work with native BK_i channels (Solaro and Lingle, 1992; Solaro et al., 1995; Herrington et al., 1995), the properties of BK_i inactivation were examined over a somewhat limited range of conditions and aspects of the steady-state inactivation properties have not been examined in detail.

Second, we compare properties of native BK_i and heterologously expressed $\alpha + \beta 2$ currents to determine to what extent the $\beta 2$ subunit is sufficient to account for properties of BK channels in chromaffin cells. The presence of the $\beta 2$ subunit message in both chromaffin cells and pancreatic β cells (Xia et al., 1999) and the correspondence of functional properties of BK_i currents and $\alpha + \beta 2$ currents has suggested that the $\beta 2$ subunit is a key molecular component

Submitted November 2, 2001, and accepted for publication December 12, 2001.

Address reprint requests to Chris Lingle, 660 S. Euclid Ave., St. Louis, MO 63110. Tel.: 314-362-8558; Fax: 314-362-8571; E-mail: clingle@morpheus.wustl.edu.

0006-3495/02/05/2448/18 $2.00

required for the inactivation behavior of the native BK_i channels, although other β subunits may also be expressed in chromaffin cells (Xia et al., 2000). However, the properties of the native BK_i currents do exhibit some differences with those described for the cloned β2 subunits (Wallner et al., 1999; Xia et al., 1999). For example, voltages of half activation ($V_{0.5}$) for native BK_i currents appear somewhat right shifted (Prakriya et al., 1996) compared to those for currents arising from coexpression of the *Slo1* α subunit with β2 subunits. These differences could reflect the possibility that BK_i channels in chromaffin cells may contain, on average, less than four β2 subunits per channel (Ding et al., 1998).

The results show that, at any Ca^{2+} up through 60 μM Ca^{2+}, a voltage can be identified at which resting inactivation is negligible, suggesting that there is no strictly Ca^{2+}-dependent inactivation. Furthermore, in the absence of Ca^{2+}, strong depolarization is sufficient to produce inactivation. Thus, although inactivation is favored by both Ca^{2+} and depolarization, consistent with conventional inactivation mechanisms in which inactivation is coupled to transitions leading to channel opening, Ca^{2+} alone is unlikely to produce the conformational changes necessary for inactivation to occur. Analysis of the ability of closed channels to inactivate also suggests that a key conformational change necessary for inactivation may precede channel opening. These properties are shared by both native BK_i currents and $\alpha + \beta$2 currents. As a consequence of the Ca^{2+} and voltage dependence of steady-state inactivation, BK channel availability can be markedly regulated at physiologically relevant voltages and $[Ca^{2+}]_i$.

METHODS

Chromaffin cell preparation

Methods of rat chromaffin cell isolation and maintenance of cultures were as described previously (Neely and Lingle, 1992; Herrington et al., 1995), based on procedures described in several earlier studies (Kilpatrick et al., 1980; Role and Perlman, 1980; Fenwick et al., 1982; Livett, 1984). Each chromaffin cell dispersion was typically done on adrenal medullas from 3–4 rats of about 2–3 months age. Whole-cell and single-channel currents were recorded 2–12 days after chromaffin cells were plated.

Oocyte removal and cRNA injection

Mature stage IV *Xenopus laevis* oocytes were prepared for injection as described in previous work (Wei et al., 1994; Xia et al., 1999). The *mSlo1* α subunit (Butler et al., 1993) construct used in initial experiments was provided by L. Salkoff (Washington Univ.) and is identical to that used in earlier work (Wei et al., 1994). The β2 auxiliary subunit is identical to that described in earlier work (Xia et al., 1999), and the β3a subunit was also described in earlier work (Xia et al., 2000). Typically, oocytes were injected with cRNA containing α:β2 subunits in a ratio of either 1:1 or 1:2 by weight. Oocytes were used 2–5 days after injection of cRNA.

Electrophysiological methods

Whole-cell currents were recorded with standard techniques (Hamill et al., 1981) with an Axopatch 1A amplifier (Axon Instruments, Foster City, CA). In whole-cell experiments, uncompensated series resistance (R_s) was typically 1.5–5 MΩ of which 80–95% was electronically compensated. In most cases, residual uncompensated R_s was less than 1 MΩ, which, for currents up to 5 nA, results in at most a 5-mV error in the effective command potential. Cell voltages during whole-cell recordings were controlled with the Clampex program from the pClamp software package (Axon Instruments). Similarly, Clampex was used to generate repetitive voltage pulse sequences to activate BK channels in single-channel recordings. Analysis of whole-cell and single-channel currents was done with our own software or with SigmaPlot (SPSS Science, Chicago, IL). Single-channel currents were recorded with an Axopatch 1C amplifier (Axon Instruments) using a 50-GΩ feedback resistor.

Solutions

The usual extracellular solution for whole-cell recordings contained the following (in mM): 150 NaCl; 5.4 KCl; 10 (*N*-(2-hydroxyethyl)piperazine-*N*′-(2-ethanesulfonic acid)) (HEPES); 1.8 $CaCl_2$, and 2.0 $MgCl_2$, pH 7.4, adjusted with *N*-methylglucamine (NMG). For whole-cell recording, for 4- and 10-μM solutions, the pipette solution contained the following in mM as described previously (Prakriya et al., 1996): 140 KCl, 20 KOH, and 10 mM HEPES(H^+), with HEDTA (*N*-hydroxyethylethylene-diaminetriacetic acid) or ethylene glycol-*bis*(β-aminoethyl ether) *N*,*N*,*N*′,*N*′-tetraacetic acid (EGTA) with added $CaCl_2$ to make the appropriate free Ca^{2+}. HEDTA, 10 mM, was used for the 60-μM [Ca^{2+}] saline, and 5 mM HEDTA for the 10-μM [Ca^{2+}] solution. EGTA, 5 mM, was used for the 4-μM [Ca^{2+}] saline. Appropriate free Ca^{2+} at a given buffer concentration was defined by the EGTAETC program (E. McCleskey, Vollum Institute, Portland, OR). Osmolarity was measured by dew point (Wescor 550 Vapor Pressure Osmometer, Logan, UT) and adjusted within 3% (internal saline, 290; external saline: 305). For experiments with elevated extracellular K^+, NaCl was replaced by equimolar substitution with KCl. For all whole-cell recordings from chromaffin cells, 200 nM apamin was added to extracellular solutions to minimize contamination by small conductance Ca^{2+}-activated K^+ currents (SK-type) (Neely and Lingle, 1992). Similarly, 200 nM tetrodotoxin was used to reduce voltage-dependent Na^+ current.

For single-channel recordings from chromaffin cells, cells were bathed in the extracellular saline used for whole-cell recordings described above. Just prior to patch excision, the solution bathing the cell was changed to the 0 Ca^{2+} saline described below. For inside-out single-channel recordings, the pipette saline contained (in mM) 140 KCl, 20 KOH, 2 $MgCl_2$, 10 HEPES, pH 7.0, adjusted with 1 N HCl. Apamin, 200 nM, was also included in the pipette solution. The cytosolic saline used during excised inside-out patch recordings was the following (in mM): 140 KCl, 20 KOH, 10 HEPES, 5 EGTA with added $CaCl_2$ to make the desired free [Ca^{2+}], pH 7.0, adjusted with 1 N HCl. HEDTA was used to buffer Ca^{2+} in solutions with desired free [Ca^{2+}] greater than 2 μM (4, 10, 60 μM). Estimates of free [Ca^{2+}] were determined as described previously (Solaro and Lingle, 1992; Solaro et al., 1997).

For most whole-cell recordings, with the Cl^--based solutions used here, the liquid junction potential primarily reflects the Na^+/K^+ gradient between pipette and bath solution. This is at most a +3 mV liquid junction potential, which was uncorrected. For measurements of the dependence of steady-state inactivation on extracellular Na^+ or K^+, the local diffusion potential resulting from switching between solutions containing 150 mM NaCl or 150 mM KCl to one containing 150 nM NMG-Cl was also measured, and found to be at most −3 mV. The results in Fig. 4 were uncorrected for this small offset.

For standard inside-out patches and whole-cell recordings, solution exchange and drug applications were accomplished with a multibarreled

perfusion tube as described previously (Herrington et al., 1995). Chemicals were from Sigma-Aldrich (St. Louis, MO).

Fast solution changes

In some experiments, we attempted to produce step changes in $[Ca^{2+}]$ at the cytosolic face of inside-out patches. We used a piezoelectric stepper (Physik Instruments, Karlsruhe, Germany) which shifted the position of a two-barrel pipette with two flowing streams of solution. A similar method has been used to study the Ca^{2+}-dependent activation of BK channels in smooth muscle cells in which changes in Ca^{2+} at the cytosolic face of inside-out patches were apparently complete within 2 ms (Markwardt and Isenberg, 1992). Using measurements of the time course of current changes resulting from changes in the salt concentration between the two streams, in our system, this method reliably produced complete changes in solution at the tip of the recording pipette in less than 2 ms. However, such changes do not reflect the changes in Ca^{2+} concentration at the face of the inside-out patch, and it is well known that pipette geometry and the details of patch formation can impact significantly on the ability of concentration changes to be produced at the surface of an inside-out patch (Cannell and Nichols, 1991). This problem is substantially more difficult for a molecule for which some active buffering may be retained by material excised with the inside-out patch. To evaluate changes in Ca^{2+} concentrations in our system, we used chromaffin cell patches in which inactivation of BK_i channels was removed with trypsin. Despite attempts to optimize our pipette shapes (Cannell and Nichols, 1991), in the best cases, application of 100 μM Ca^{2+} (unbuffered) resulted in current activation with a 10–90% rise time of only 34.3 $\pm$ 4.7 msec. With a buffered 10-μM Ca^{2+} solution (5 mM HEDTA), similar rise times were also achieved. Such exchange times are not adequate to allow direct visualization of the activation time course of BK channels. However, for the experiments reported here, our only requirement was that the response to the change in Ca^{2+} be identical between different applications. Despite the limitations of this method, it allowed us to examine some properties of inactivation under conditions not accessible with other methods.

Data analysis

Currents or extracted data were fit using a Levenberg–Marquardt search algorithm to obtain nonlinear least-squares estimates of function parameters. When given, 90% confidence limits define the range over which there is a 90% probability that the true value may be found. Steady-state inactivation curves were fit with the following form of a Boltzmann function:

$$f(V) = \frac{f_{max}}{1 + \exp^{(V - V_{0.5})/k}}, \quad (1)$$

where f_{max} is the limiting fractional availability of current, $V_{0.5}$ is the voltage of half availability, and k is the voltage-dependence of the distribution in millivolts.

RESULTS

Properties of steady-state inactivation of native BK_i currents in chromaffin cells

The steady-state availability of BK_i channels for activation as a function of different conditioning potentials and $[Ca^{2+}]_i$ was examined in both whole-cell and single-channel recordings. In whole-cell recordings from chromaffin cells, currents were examined with pipette $[Ca^{2+}]$ buffered to 4, 10, or 60 μM. Cells were held at -60 mV before stepping to different conditioning potentials for 3 s. The period of time at the conditioning potential was sufficient to allow channels to reequilibrate to a new steady-state condition at the conditioning potential as determined from the voltage- and Ca^{2+}-dependence of the recovery time course (J. P. Ding and C. J. Lingle, in preparation). Figure 1 *A*

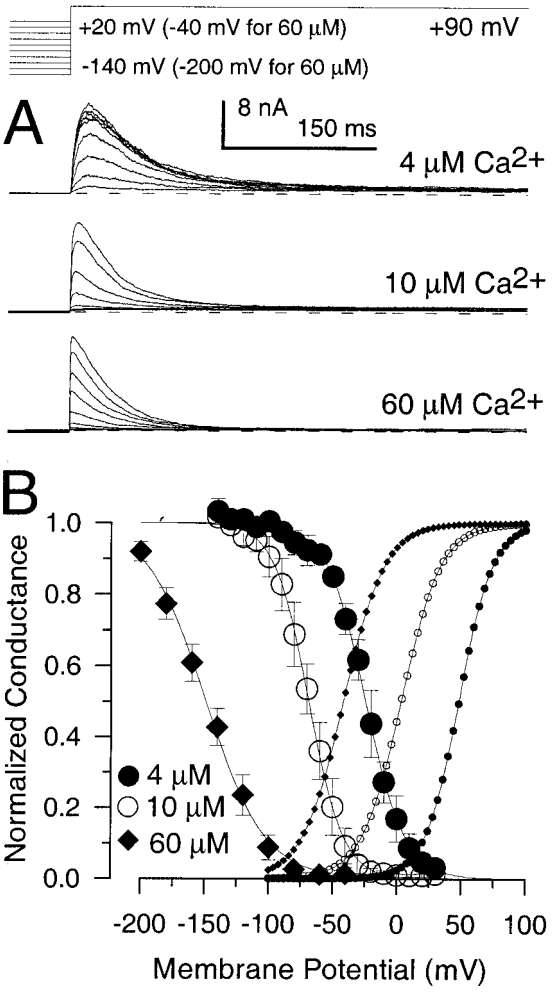

FIGURE 1 Steady-state inactivation properties of BK_i channels in chromaffin cells. (*A*) The fractional availability of BK_i channels for activation as a function of conditioning potential was determined with the indicated voltage protocol. The conditioning-step duration was 3 s. For 4 and 10 μM Ca^{2+}, the conditioning steps ranged from -140 to $+20$ mV in 10-mV increments, whereas for 60 μM Ca^{2+}, the conditioning steps ranged from -200 mV to -40 mV in 10-mV increments. Currents elicited by this protocol are shown for three different cells in which cytosolic Ca^{2+} was buffered to 4, 10, and 60 μM, respectively, from top to bottom as indicated. The extracellular solution contained 5.4 mM K^+. (*B*) The normalized fractional availability curves for 4 (●; 3 cells), 10 (○; 5 cells), and 60 μM (◆; 3 cells) Ca^{2+} are plotted. In each case, the solid lines are a fit of the Boltzmann function given by Eq. 1. Fitted values for $V_{0.5}$ were -24.1 ± 0.8, -68.6 ± 0.6, -148.8 ± 4.7 mV for 4, 10, and 60 μM, respectively, while values for k were -15.3, -13.6, and -23.0 mV. Curves for activation of conductance at 4, 10, and 60 μM Ca^{2+} obtained with identical solutions (Prakriya et al., 1996) are also shown for comparison.

shows currents activated at +90 mV following various conditioning potentials for three different cells with 4, 10, or 60 μM pipette Ca^{2+}. Peak current elicited at +90 mV from each conditioning potential was normalized to the peak current elicited from the most negative conditioning potential (Fig. 1 *B*). For each $[Ca^{2+}]$, the fractional availability plot was fit with a single Boltzmann (Eq. 1). With 4 μM Ca^{2+} (3 cells), the voltage of half availability ($V_{0.5}$) was -15.3 ± 0.7 mV ($k = -24.1$ mV). At 10 μM Ca^{2+} (5 cells), $V_{0.5} = -68.6 \pm 0.6$ mV ($k = -13.6$ mV). At 60 μM (3 cells), $V_{0.5} = -148.8 \pm 4.1$ mV ($k = -23.0$ mV).

For comparison, conductance–voltage curves for activation of BK conductance obtained in our earlier work from whole-cell recordings on rat chromaffin cells (Prakriya et al., 1996) are also shown. As with many other inactivating voltage-dependent channels, when fractional availability curves are compared to activation curves at a given $[Ca^{2+}]$, inactivation of BK_i channels is substantial at potentials where activation of BK_i current is minimal.

In the whole-cell experiments just described, it is not possible to determine whether the limiting channel availability at negative potentials is comparable at different $[Ca^{2+}]$, because only a single $[Ca^{2+}]$ is examined for each cell. Therefore, the steady-state availability of BK_i current for activation was also examined in multichannel patches from rat chromaffin cells. Patches were held at −40 mV and then stepped for 100–200 ms to potentials between −200 and 0 mV, before an activation step usually to +80 mV at Ca^{2+} concentrations of 4, 10, and 60 μM (Fig. 2 *A*). For a given $[Ca^{2+}]$ and conditioning voltage, this stimulation protocol was repeated 20–90 times to generate an ensemble average. To ensure patch viability, the conditioning potentials were somewhat shorter than required to produce a true steady-state condition at the more positive conditioning potentials. This would result in a small flattening of the fractional availability curve, with points generated at conditioning potentials positive to the holding potential (−40 mV) overestimating the true availability.

An example of the fractional BK_i availability from the multichannel patch shown in Fig. 2 *A* is plotted in Fig. 2 *B* for 4, 10, and 60 μM. Each point represents a separate ensemble average. A single Boltzmann (Eq. 1) was fit to each set of points to estimate the voltage of half availability. At 60, 10, and 4 μM, respectively, the voltage of half availability was -149.2 ± 8.8 mV (mean ± SD for 3 patches), -78.4 ± 22.7 mV (for 4 patches), and -13.4 ± 1.4 mV (for 3 patches). These numbers are similar to the whole-cell estimates described above, although it should be noted that, in the patch experiments, channels were studied with symmetrical K^+ solutions.

An important question is whether the limiting fraction of channel availability at the most negative potentials is similar at each $[Ca^{2+}]$. For both whole-cell and patch measurements (Figs. 1 and 2), for each $[Ca^{2+}]$, at sufficiently negative potentials, additional negative steps in voltage had

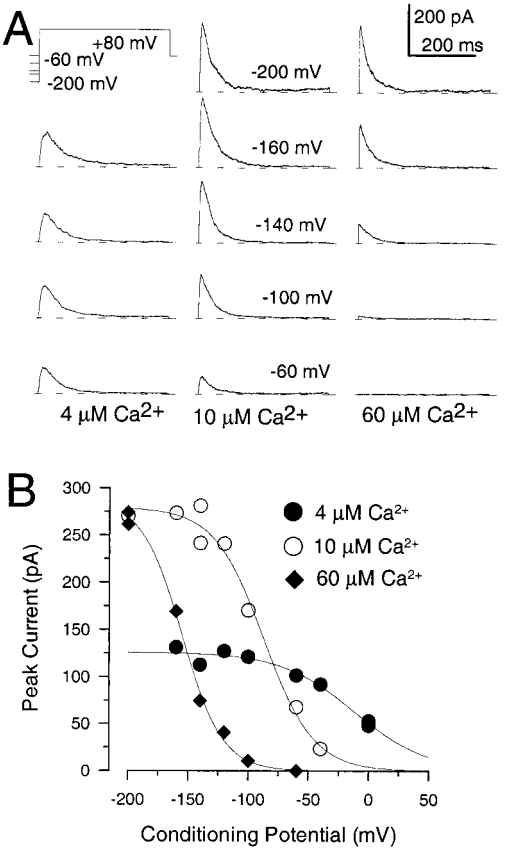

FIGURE 2 Fractional availability of BK_i channels in inside-out patches suggest a similar maximal limiting availability $[Ca^{2+}]$ is elevated. (*A*) Traces show ensemble current averages obtained from an inside-out patch during steps to +80 mV following a 200-ms conditioning step to potentials between −200 and −60 with either 4 μM (*left column*), 10 μM (*middle column*), or 60 μM (*right column*) Ca^{2+}. Each ensemble is the average of 25–90 individual sweeps. (*B*) Fractional availability curves obtained at 4, 10, and 60 μM for the patch shown in (*A*) are shown. The solid lines are fits of Eq. 1. At 4 μM Ca^{2+}, $V_{0.5} = -7.04$ mV ($k = -35.3$ mV); at 10 μM, $V_{0.5} = -85.8$ mV ($k = -21.3$ mV); and, at 60 μM Ca^{2+}, $V_{0.5} = -155.53$ mV ($k = -18.0$ mV). Currents are plotted.

no influence on the steady-state availability. Over this range of voltages, one can therefore ask the question of whether there is any indication that there is some specific Ca^{2+}-dependent inactivation process. Estimates of fractional availability were combined for the three patches in which a sufficient number of ensemble averages were generated at the three concentrations of 4, 10, and 60 μM. From the fit of a single Boltzmann to the averaged data, the limiting channel availability at negative potentials with 4 μM was ~28% of that at 60 μM, whereas the limiting availability at 10 μM was ~87% of that at 60 μM. Thus, it is clear that the limiting availability at 10 μM Ca^{2+} does not exceed that at 60 μM. This would argue that, at least at $[Ca^{2+}]$ up to 60 μM, there is no strictly Ca^{2+}-dependent inactivation process.

Why does the limiting availability appear less at 10 and 4 μM than at 60 μM? The likely explanation is that differ-

ences in activation kinetics at +90 mV for the three concentrations affect the peak amplitude in two ways: first, there may be a differential amount of inactivation prior to the time of peak current activation and, second, with a faster activation rate (i.e., at 60 μM) there will be more synchrony in channel activation than with slower activation rates (i.e., at 4 μM). The differences in time to peak current activation with different [Ca^{2+}] are apparent in the records of Figs. 1 and 2.

The steady-state inactivation behavior of $\alpha + \beta 2$ currents is generally similar to that of BK_i currents

Steady-state fractional availability curves for heterologously expressed $\alpha + \beta 2$ currents were also measured in a set of four patches as shown in Fig. 3. Each inside-out patch was exposed to 4, 10, and 60 μM Ca^{2+} (Fig. 3 *A*) and fractional availability curves were generated (Fig. 3 *B*) as above. Qualitatively, the results were quite comparable to those obtained with native BK_i currents, although the $V_{0.5}$ at a given Ca^{2+} was shifted to more negative potentials. Again, the maximal available current was greater at 60 μM than at either 4 or 10 μM, suggesting that the peak of current in 4 or 10 μM is limited for reasons already given. Average values from four patches are displayed on Fig. 4 *D*. As [Ca^{2+}] is increased, the fractional availability of BK_i current is shifted to more negative potentials. Up to 60 μM Ca^{2+}, we find no evidence for a limiting $V_{0.5}$ for fractional availability.

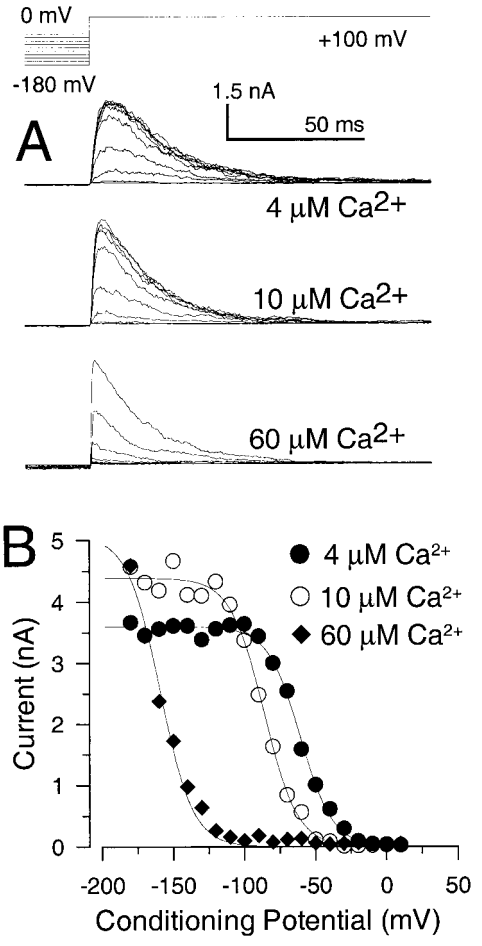

FIGURE 3 Steady-state inactivation properties of $\alpha + \beta 2$ currents. (*A*) The indicated voltage protocol was used to determine fractional availability of $\alpha + \beta 2$ currents expressed in *Xenopus* oocytes. From a holding potential of 0 mV, the patch was stepped to potentials between −180 and +10 mV for 3 s before a test step to +100 mV. The patch was sequentially bathed in 4, 10, and 60 μM Ca^{2+} as indicated. (*B*) From the patch shown in (*A*), peak current activated at +100 mV is plotted as a function of conditioning potential for 4 (●), 10 (◇), and 60 (◆) μM Ca^{2+}. Solid lines are fits of Eq. 1. For 4 μM Ca^{2+}, I_{max} = 3.6 nA, k = −11.37 mV, and $V_{0.5}$ = −60.8 mV; for 10 μM, I_{max} = 4.4 nA, k = −11.61 mV, and $V_{0.5}$ = −86.15 mV; for 60 μM, I_{max} = 5.1 nA, k = −11.4 mV, and $V_{0.5}$ = −159.2 mV.

Steady-state inactivation depends on both extracellular Na^+ and K^+

In experiments above, steady-state inactivation in whole-cell experiments was studied with physiological ionic gradients, whereas in the inside-out patch experiments, currents were studied with symmetrical K^+. Despite this difference, the $V_{0.5}$ for fractional availability at different [Ca^{2+}] was quite similar for the two sets of experiments. To examine this directly, the dependence of steady-state inactivation on changes in the concentration of K^+ or Na^+ was examined by replacing either ion with *N*-methyl glucamine. In these experiments, single chromaffin cells were studied with 10 μM pipette Ca^{2+} using protocols identical to those used in Fig. 1. The dependence of BK_i current availability on conditioning potential at different extracellular [K^+] is plotted in Fig. 4 *A*. At 150 mM K^+, the $V_{0.5}$ for current availability is ∼−80 mV, similar to the measurements described above. However, as [K^+] is decreased, the $V_{0.5}$ shifts markedly to more negative potentials, being negative to −125 mV at 5.4 mM K^+. This seems surprising given that, in the experiments with physiological ionic gradients, the $V_{0.5}$ at 10 μM Ca^{2+} was around −80 mV. We, therefore, examined the dependence of steady-state inactivation on changes in extracellular Na^+ (Fig. 4 *B*). Similar to the experiments with K^+, the $V_{0.5}$ for current availability underwent a marked leftward shift as the concentration of extracellular Na^+ was diminished.

The dependence of the $V_{0.5}$ for fractional current availability is plotted as a function of the monovalent cation concentration in Fig. 4 *C*. The concentration of K^+ producing about half the full effect was ∼3 mM, whereas for Na^+, it was ∼33 mM. Despite the fact that K^+ is more effective at producing this shift, at 150 mM of either cation, the effects are largely the same. The similarity in effect of 150 mM of either cation probably accounts for the fact that the

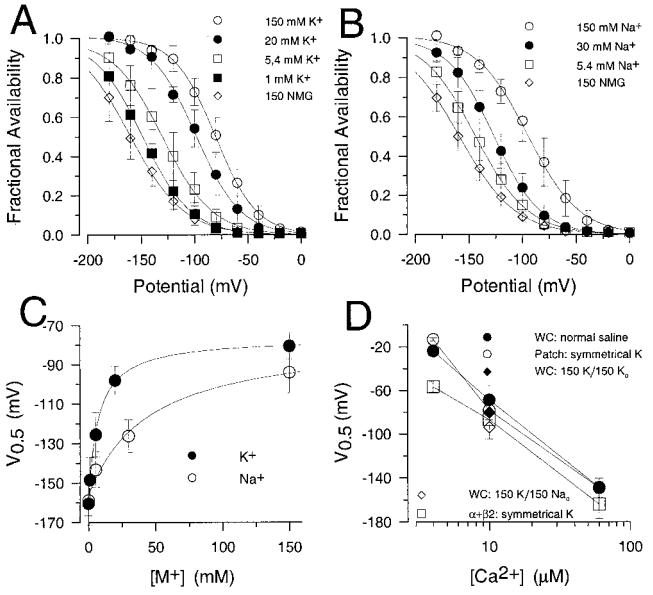

FIGURE 4 Dependence of steady-state inactivation on identity and concentration of extracellular monovalent cation. (*A*) Steady-state fractional availability curves were generated as in Fig. 1 in whole-cell recordings from rat chromaffin cells with 10-μM pipette Ca^{2+}. The extracellular solutions contained various concentrations of K^+ with added NMG to keep the osmolarity near 300. Curves are fits of Eq. 1 with $V_{0.5}$ values of -160.3, -148.2, -129.5, -98.5, and -80.3 mV for 0, 1, 5.4, 20, and 150 mM K^+, respectively. (*B*) Steady-state fractional availability curves were generated with various extracellular Na^+ concentrations. $V_{0.5}$ values were -158.4, -143.8, -126.2, and -94.9 for 0, 5.4, 30, and 150 mM Na^+, respectively. (*C*) $V_{0.5}$ values from (*A*) and (*B*) are plotted as a function of the respective monovalent cation concentration. Solid lines are fits of $V_{0.5} = V_{min} + \{[K]_o/([K]_o + K_D)\}\Delta V$ where V_{min} is the $V_{0.5}$ with no Na^+ or K^+, K_D is the concentration of half maximal effect and ΔV is the maximum change in $V_{0.5}$ at saturating cation concentrations. For K^+, the K_D was 7.4 mM, whereas, for Na^+, the K_D was 45.9 mM. The limiting $V_{0.5}$ at saturating $[M^+](V_{min} + \Delta V)$ was -76.4 mV for K^+ and -75.5 mV for Na^+. (*D*) $V_{0.5}$ is plotted as a function of Ca^{2+} for estimates obtained from normal physiological gradients in whole-cell experiments (Fig. 1), from ensemble averages in excised patch experiments (Fig. 2) with symmetrical K^+, and, at 10 μM, for whole-cell experiments in which the extracellular monovalent cation was either 150 mM K^+ (*panel A*) or 150 mM Na^+ (*panel B*).

steady-state inactivation properties appear similar when studied either with symmetrical K^+ solutions (Figs. 2 and 3) or with physiological ionic gradients (Fig. 1). In both cases, the total concentration of extracellular monovalent cation was similar.

One surprising aspect of these results is that extracellular Na^+ influences the steady-state current availability. In previous work using similar solutions, we showed that extracellular Na^+ does not appreciably influence the rates of recovery from inactivation of BK_i channels in chromaffin cells (Solaro et al., 1997). One explanation of the ability of an extracellular ion to shift steady-state inactivation would be that it would influence either the rates of onset or recovery from inactivation. The rightward shift in fractional availability curves with increases in $[K^+]_o$ is qualitatively consistent with an increase in recovery from inactivation seen with increases in $[K^+]_o$ (Solaro et al., 1997). However, the fact that $[Na^+]_o$ does not influence recovery from inactivation suggests that extracellular ions may influence steady-state inactivation properties in other ways, perhaps by effects on the voltage-dependence of channel activation that then impact on steady-state inactivation (Demo and Yellen, 1992; Piskorowski and Aldrich, 2001). This issue will require further investigation.

Figure 4 *D* summarizes the relationship between steady-state inactivation $V_{0.5}$ and $[Ca^{2+}]$ determined from a variety of experimental approaches and for both BK_i currents and $\alpha + \beta 2$ currents. Estimates for $\alpha + \beta 2$ currents are shifted to somewhat more negative potentials compared to BK_i currents, whereas estimates of $V_{0.5}$ for BK_i currents were comparable whether measured by whole-cell recordings, single channel patches, or with different ionic gradients.

At negative potentials and 10 μM Ca^{2+}, there is little resting inactivation

Experiments above suggest that, at negative potentials, a similar fraction of channels may be available for activation at 10 and 60 μM, suggesting no strictly Ca^{2+}-dependent component of inactivation. To examine this more closely and to define the true limiting fractional availability of BK_i channels, the probability that a single channel will open during a step to +60 mV was examined from different conditioning potentials for six patches from rat chromaffin cells. Because the multichannel patch experiments suggested that the limiting availability for 10 and 60 μM was not markedly different, the single-channel patches were only studied with 10 μM to avoid the extreme potentials required to define availability with 60 μM. Representative sweeps from a single-channel patch exposed to 10 μM Ca^{2+} with three different conditioning potentials, -60, -100, and -140 mV are shown in Fig. 5 *A*. The ensemble averages from the single channel sweeps are shown below. The peak probability of being open (P_o) determined from the peak of the ensemble average current was 0.18, 0.48, and 0.85 for -60, -100, and -140 mV, respectively. In contrast, the probability that a burst of openings was observed during the step to +60 mV was 0.255 (26 out of 102 sweeps) from a -60-mV conditioning step, 0.581 (61 out of 105 sweeps) from -100 mV, and 0.91 (153 of 168 sweeps) and 0.874 (93 of 95 sweeps) for two sets of sweeps from -140 mV. In each case, the peak current underestimates the true probability of opening because of asynchrony of channel activation, consistent with the idea that asynchrony in channel opening will result in underestimates of the true fractional availability particularly at lower $[Ca^{2+}]$. The voltage-dependence of the probability that an opening would occur following a particular conditioning potential is plotted for this patch in Fig. 5 *B*. The voltage at which

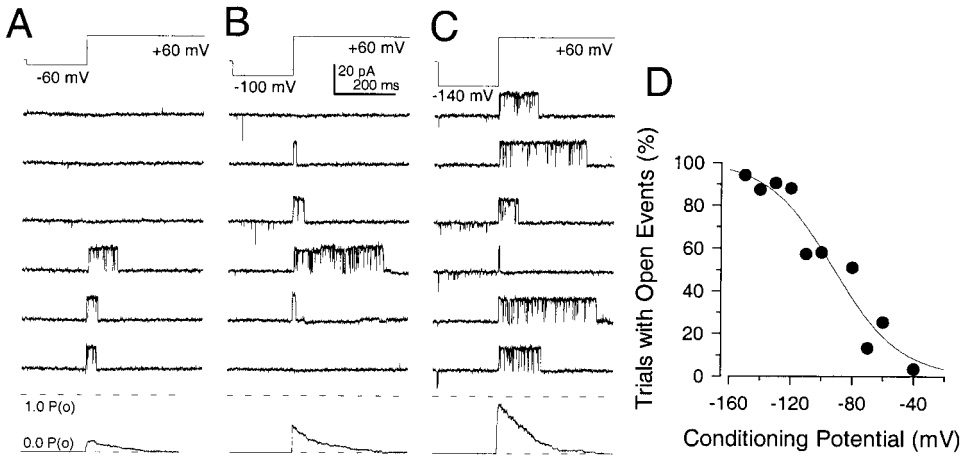

FIGURE 5 At sufficiently negative potentials, there is essentially no resting inactivation of BK_i channels. An inside-out single channel patch from a chromaffin cell was bathed with 10 μM Ca^{2+}. Channel activation at +60 mV was examined following a 200-ms conditioning step to (*A*) −60 mV, (*B*) −100 mV, or (*C*) −140 mV. The average of detected openings for (*A*) 103, (*B*) 108, and (*C*) 64 sweeps are shown below the individual traces. (*D*) The percentage of sweeps in which the BK channel opened during the step to +60 mV is plotted against the conditioning potential. The solid line is a fit of Eq. 1 where $V_{0.5}$ is −92.9 ± 6.3 mV and k is −21.0 ± 6.4 mV.

a channel is likely to open during half of the steps to +60 mV was −92.9 mV, comparable to the values obtained both in whole-cell recordings and in multichannel patches.

For a set of nine runs of consecutive sweeps obtained from six patches with conditioning potentials of −130, −140, or −150 mV, the mean limiting probability that an opening will occur at +60 mV was 0.82 ± 0.07. This number probably underestimates the true limiting channel availability for three reasons. First, the conditioning step duration was 100 ms, which, because of a slow component of recovery from inactivation, is not quite sufficient to reach a full steady-state condition. Second, in experiments in which inactivation was removed by trypsin application, the saturating open probability at +60 mV with 10 μM Ca^{2+} was typically only ~90–95%. This reflects the occurrence of long-lived closures, many of which persist through the complete duration of a 400-ms voltage step and may span several sweeps. Thus, occupation by channels of such long-lived closed states, which are distinct from the rapid inactivation process under evaluation here, should be excluded from a consideration of whether channel availability is limited by persisting resting rapid inactivation. Third, it is also likely that some underestimate in the limiting probability of opening will occur at +60 mV with 10 μM, because some channels may inactivate at +60 mV before ever opening. Therefore, at 10 μM Ca^{2+} and potentials of −140 mV or more negative, a BK_i channel will rarely occupy an inactivated state corresponding to the rapid inactivation process. Because the experiments with multichannel patches showed that the limiting fractional availability with 60 μM Ca^{2+} was at least that with 10 μM Ca^{2+}, this again argues that, at sufficiently negative potentials, there is no residual strictly Ca^{2+}-dependent inactivation, with Ca^{2+} concentrations up through 60 μM.

The onset of inactivation and steady-state inactivation properties in 0 Ca^{2+}

We next examined to what extent inactivation can occur in the absence of Ca^{2+}. The 0 Ca^{2+} solutions contained 5 mM EGTA. Even assuming a contaminant concentration of 20 μM Ca^{2+}, this should result in free Ca^{2+} of no more than ~1 nM. At this concentration, the occupancy of Ca^{2+} binding sites involved in activation of BK channels is thought to be negligible (Cox et al., 1997). The onset of inactivation in 0 Ca^{2+} was investigated in two ways. First, we used standard activation protocols to positive potentials to examine the properties of the BK_i channels in chromaffin cells. Because of the large depolarizations required, the small amount of current, and the need to average a reasonable number of sweeps, patches from chromaffin cells suitable for this experiment were difficult to achieve. However, in a few cases, successful patches showed that channels activated in 0 Ca^{2+} exhibit clear inactivation. Although the apparent rates of inactivation over most potentials are slow compared to those observed with more elevated [Ca^{2+}] (Fig. 6 *A*), at the most positive potentials, the apparent inactivation time constant (τ_i) approached a value similar to the limiting τ_i that has described in other work (Solaro and Lingle, 1992; Solaro et al., 1997), being near 20–30 ms. Similar experiments were done with α + β2 currents in inside-out patches from oocytes (Fig. 6 *B*). Again, at the most positive activation potentials, τ_i in 0 Ca^{2+} approached values similar to those seen in 10 μM Ca^{2+} (Fig. 6, *C* and *D*). This is consistent with the

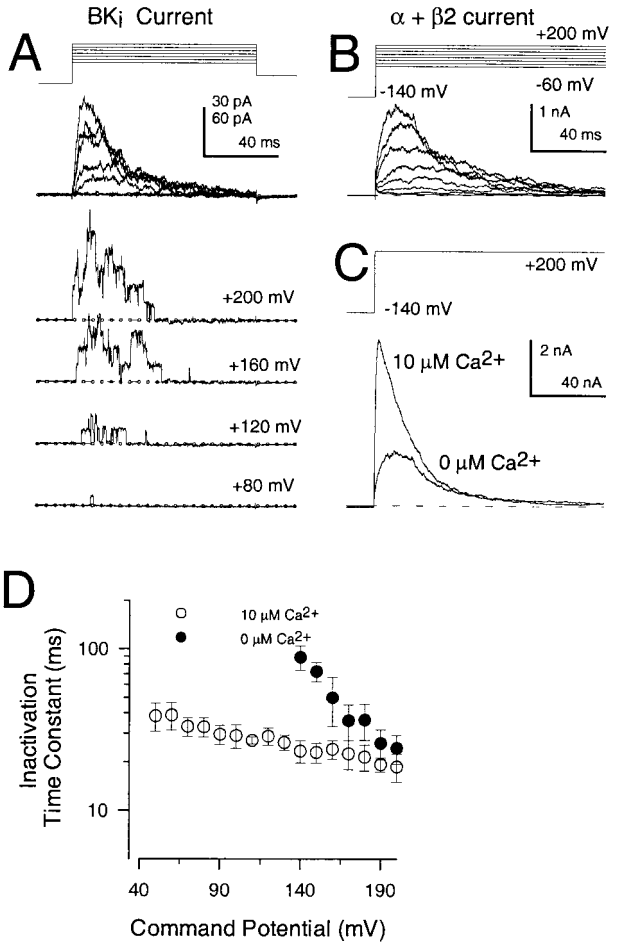

FIGURE 6 At positive potentials, inactivation approaches the same limiting rates even in the absence of Ca^{2+}. (*A*) An inside-out patch from a chromaffin cell was bathed with 0 Ca^{2+} saline. Traces show examples of single sweeps of channels activated at the indicated potentials following a 200-ms conditioning step to −140 mV. Each sweep was taken from a set of similar sweeps that were used to generate the current averages shown at the top. At the most positive activation potentials, despite the broad time course of activation of channels in 0 Ca^{2+}, the channels in the patch exhibit clear inactivation. From the current averages, at the most positive potentials, the inactivation time constant approaches 20–25 ms. (*B*) Traces display $\alpha + \beta 2$ currents from an inside-out patch from an oocyte to show the inactivation time course with 0 Ca^{2+}. (*C*) $\alpha + \beta 2$ current activated at +200 mV is compared for 10 μM Ca^{2+} and 0 Ca^{2+} to show the similarity in inactivation time course. (*D*) The inactivation time constants measured from current averages as in (*B*) are plotted as a function of command potential for $\alpha + \beta 2$ currents. For comparison, τ_i measured at 10 μM is also shown to emphasize that, at the most positive potentials, τ_i obtained in 0 Ca^{2+} approaches that observed for 10 μM Ca^{2+}.

observation that τ_i with 500 nM Ca^{2+} was similar to that measured with 10 μM Ca^{2+} at +130 mV for $\alpha + \beta 2$ currents in oocytes (Wallner et al., 1999). These results suggest that, with sufficiently positive voltages, BK_i channels in chromaffin cells and cloned $\alpha + \beta 2$ channels inactivate as readily without Ca^{2+} as with Ca^{2+}.

Because of the possibility that inactivation might regulate BK_i channel availability, we were also interested in the extent and rate of inactivation that might occur in 0 Ca^{2+} saline at more modest voltages. For BK_i channels in chromaffin cells, the small amplitude of currents activated with 0 Ca^{2+} precluded the use of more conventional procedures. Therefore, to examine inactivation that occurs in 0 Ca^{2+} saline at potentials negative to +100 mV, we attempted to examine the effects of conditioning potentials in 0 Ca^{2+} saline on the subsequent currents activated by a step change in [Ca^{2+}] at a given command potential. Such a method poses many challenges (see Methods), one being that it is difficult to rapidly change concentrations in inside-out patches (e.g., Cannell and Nichols, 1991). However, as long as the time course of the change in [Ca^{2+}] is identical among applications, because here we are only interested in the effect of the conditioning potential on that response, the rapidity of the change in [Ca^{2+}] is not so critical. Using this procedure, patches were continuously perfused with 0 Ca^{2+} saline at various conditioning potentials. Coincident with a depolarizing voltage step, the solution bathing the patch was then changed to one containing either 10 or 100 μM Ca^{2+} (Fig. 7 *A*). Using this procedure, the ability of various potentials to produce inactivation of BK_i channels in 0 Ca^{2+} was defined (Fig. 7 *B*). This procedure revealed that, at steady-state, about half the channel population is inactivated at ~+40 to +50 mV. Similar results were obtained whether [Ca^{2+}] was stepped to either 10 or 100 μM. Using this method, the onset of inactivation in 0 Ca^{2+} was also examined (Fig. 7 *C*) by varying the time of the step to 100 μM Ca^{2+} following imposition of a given conditioning potential. This experiment also confirmed that inactivation is appreciable with 0 Ca^{2+} at potentials between +40 and +80 mV with the approach to steady-state inactivation occurring over hundreds of milliseconds (Fig. 7 *D*). In 0 Ca^{2+}, there appears to be little resting inactivation at potentials negative to ~+20 mV. However, by +50 mV, half the channel population is inactivated in 0 Ca^{2+} at steady-state conditions.

We next examined the properties of steady-state inactivation and the onset of inactivation in 0 Ca^{2+} with $\alpha + \beta 2$ currents. Because robust $\alpha + \beta 2$ currents could be elicited with 0 Ca^{2+} saline, more conventional procedures for looking at inactivation onset and steady-state inactivation were used. Conditioning steps to potentials between 0 and +80 mV were applied for durations up to 560 ms, prior to a subsequent test step to +200 mV (Fig. 8 *A*). The fractional reduction in peak current was plotted as a function of conditioning-step duration (Fig. 8 *B*) and it can be seen that channels inactivate with time constants on the order of hundreds of milliseconds with somewhat less than half the population of channels being inactivated at +60 mV, whereas ~70% are inactivated at steady-state at +80 mV. Steady-state inactivation was also measured in individual patches bathed with 0 Ca^{2+} saline yielding a voltage of half inactivation of +60 mV.

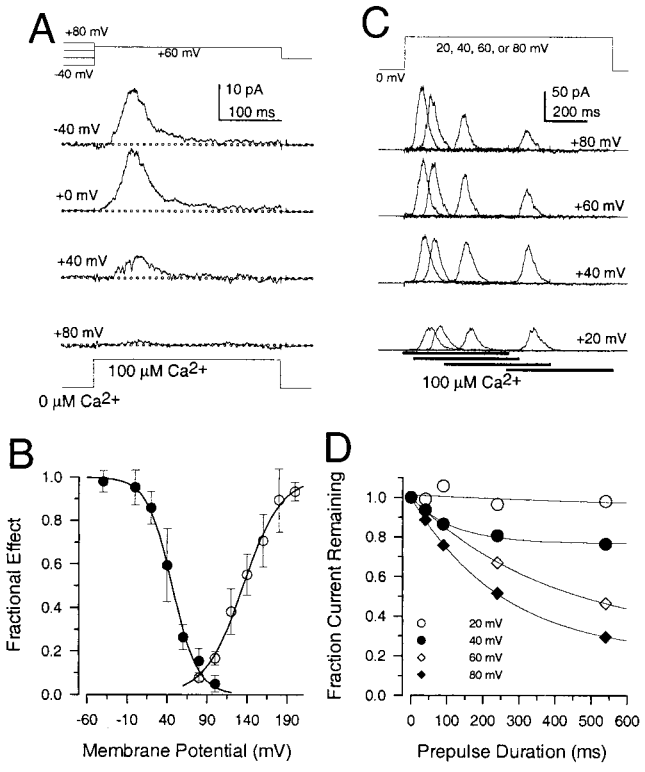

FIGURE 7 Steady-state inactivation and onset of inactivation in 0 Ca^{2+}. (*A*) An inside-out patch from a rat chromaffin cell was continuously perfused with 0 Ca^{2+} saline. The patch was held at various conditioning potentials (as indicated in the stimulation protocol on the top and listed on the figure) and then stepped to +60 mV, at which time the patch was exposed to a solution containing 100 μM Ca^{2+}. As the conditioning potential was made more positive, there is a larger reduction in current activated by 100 μM Ca^{2+}. This reduction reflects the amount of inactivation that occurred in 0 Ca^{2+}. (*B*) The fractional availability of BK current from experiments such as that shown in (*A*) is plotted (●) as a function of the conditioning potential. Half-maximal availability determined from a fit of Eq. 1 (*solid line*) was 46.3 ± 3.1 mV (k = −16.1 + 2.6 mV). For comparison, activation of peak BK_i conductance in response to a step change to 100 μM Ca^{2+} (Fig. 5 *A*) is plotted (○) as a function of command potential. The solid line is also a fit of Eq. 1, with $V_{0.5}$ = 135.2 mV. (*C*) An inside-out patch was held at 0 mV with 0 μM Ca^{2+}. Following a step to either +20, +40, +60, or +80 mV (as indicated by the traces), the patch was then exposed at various times (0, 50, 200, or 500 ms) following the voltage step to 100 μM Ca^{2+} (as indicated by the horizontal bars below the traces). At +20 mV, there is little reduction in the current activated by 100 μM over the 500-ms period in 0 Ca^{2+}, whereas, at more positive potentials, there is appreciable inactivation in 0 Ca^{2+} within 500 ms. (*D*) The fraction of current activated by 100 μM Ca^{2+} is plotted as a function of the time preceding the Ca^{2+} step. The solid lines are the fits of an exponential function to each set of points. At +40 mV, τ_i = 116.6 ms; at +60 mV, τ_i = 395.6 ms; and, at +80 mV, τ_i = 254.4 ms. The fractional current availability predicted from the exponential fit in each case was 0.77, 0.28, and 0.20 for +40, +60, and +80 mV, respectively. These values are generally consistent with those plotted in Fig. 8 *B*.

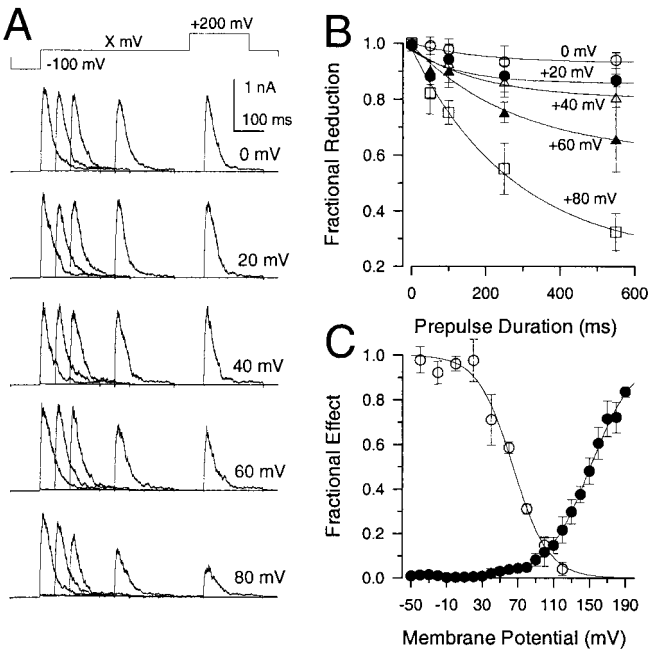

FIGURE 8 Steady-state inactivation and inactivation onset for $\alpha + \beta 2$ currents. (*A*) The indicated voltage-protocol (one sweep shown), was used to examine the effect of conditioning voltage and duration on the ability of 0 Ca^{2+} to cause inactivation of current elicited by a subsequent test step to +200 mV. Each current trace corresponds to an average of 9 sweeps. (*B*) The fractional reduction of the current elicited at +200 mV is plotted as a function of conditioning-step duration. Each point is the mean ± SD of four patches. Solid lines are single exponential fits to the inactivation time course with τ_i of 178.8, 130.4, 193.6, 282.3, and 279.2 ms, for 0 through +80 mV, respectively. (*C*) The voltage-dependence of activation of peak $\alpha + \beta 2$ current obtained in 0 Ca^{2+} (●; 4 patches) and the voltage-dependence of steady-state inactivation obtained in 0 Ca^{2+} (○; 5 patches) are plotted for $\alpha + \beta 2$ currents. From Eq. 1, half activation occurred at 151 mV, whereas, in 0 Ca^{2+} at steady-state, half the channels are inactivated at 64.5 mV.

The onset of inactivation of BK_i current in the range of physiological potentials

Experiments above suggest that, with sufficiently low [Ca^{2+}], at physiological resting potentials, there should be little resting inactivation of BK_i channels. However, the release of Ca^{2+} from cytosolic stores may transiently elevate bulk cytosolic Ca^{2+} into the micromolar range (Herrington et al., 1995), such that substantial inactivation of BK_i current may occur. Here, using chromaffin cells, we examine the onset of inactivation at potentials negative to 0 mV with either 2 or 10 μM Ca^{2+}. For this, we used a protocol in which we measured the fractional reduction in current activated at +90 mV by a conditioning step to various potentials (e.g., −40, −60, −80, or −100 mV) of varying durations (Fig. 9 *A*). This was done using whole-cell recordings with 10 μM pipette Ca^{2+}. Because, with this protocol, only a relatively limited set of points describes the inactivation time course, kinetic complexities in the inactivation process may be obscured. Over all voltages, inactivation proceeded in an approximately exponential time course (Fig. 9 *B*), although, at some potentials, two exponential components gave a better description of the inactivation time course. The steady-state level of current (Fig.

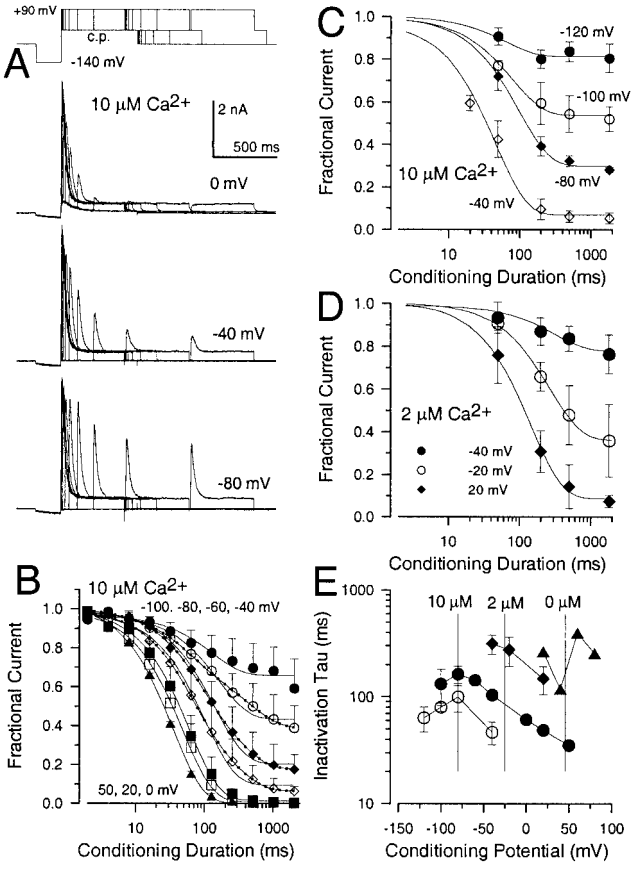

FIGURE 9 The onset of inactivation at negative potentials. (*A*) BK currents were elicited in a rat chromaffin cell with 10 μM pipette Ca^{2+} with physiological K^+ gradients. Following a 200-ms step to −140 mV, a conditioning step of variable duration was applied to either 0 mV (*top current traces*), −40 mV (*middle traces*), or −80 mV (*bottom traces*) prior to a test step to +90 mV to elicit robust BK current activation. The step to 0 mV results in rapid and complete inactivation, whereas the steps to −80 mV result in slower and less complete inactivation. (*B*) The fractional inactivation as a function of conditioning-step duration is plotted for experiments as in (*A*) for −100, −80, −60, −40, 0, 20, and 50 mV conditioning potentials. Solid lines are single exponential fits with τ_i of 131.8, 162.9, 142.7, 103.9, 61.1, 48.7, and 35.2 ms for −100 through 50 mV, respectively. Half maximal inactivation for this set of cells occurred around −80 mV, consistent with earlier results. For inactivation onset at −80, −60, and −40 mV, a double-exponential fit (*lines with smaller dots*) resulted in a substantially better fit to the data. The faster inactivation component (fitted value ±90% confidence limit with amplitude of fast component in parentheses) was 54.0 ± 15.8 (44.8%), 74.1 ± 19.7 (51.4%), and 58.5 ± 10.5 (59.4%) ms, for −80, −60, and −40 mV, respectively, with a slow component of 458.6 ± 134, 310.0 ± 99.1, and 271.4 ± 80.4 ms. (*C*) The onset of inactivation at 10 μM Ca^{2+} was measured for BK_i channels in excised patches from rat chromaffin cells using a protocol similar to that in (*A*). Solid lines are fits of a single-exponential function to the inactivation time course with τ_i of 46.7, 99.5, 79.7, and 63.2 ms, for −40, −80, −100, and −120 mV, respectively. Half inactivation occurs between −80 and −100 mV. (*D*) The onset of inactivation was measured in inside-out patches using 2 μM Ca^{2+}. τ_i was 148.1, 275.4, and 314.8 ms, for 20, −20 mV, respectively. (*E*) τ_i is plotted as a function of inactivation potential for excised patches at 0 (▲), 2 (◆), and 10 (○) μM Ca^{2+}, and also at 10 μM (●) for whole-cell recordings. Vertical lines indicate estimates of voltages of half-availability at 0, 2, and 10 μM Ca^{2+}.

9 *B*) achieved in such experiments correlates well with the steady-state inactivation experiments shown above, indicating that at a potential somewhat negative to −80 mV half the BK_i channel population in chromaffin cells becomes unavailable for activation with 10 μM Ca^{2+}.

The onset of inactivation was also examined in excised inside-out patches (symmetrical K^+ solutions) with either 2 μM or 10 μM Ca^{2+} (Fig. 9, *C* and *D*) using a similar procedure. τ_i for 2 and 10 μM Ca^{2+} is plotted in Fig. 9 *E*, along with estimates for 0 Ca^{2+} (Fig. 6 *D*). These results indicate that, at 10 μM Ca^{2+}, τ_i at potentials negative to 0 mV is in the range of 50–200 ms, whereas, even at 2 μM, τ_i is less than 400 ms at −20 and −40 mV. These values for τ_i should not be viewed as indicative of the molecular rates of the inactivation transitions, because the rate of entry into inactivated states under these conditions most certainly reflects coupling to other transitions in the activation of the channel.

These estimates of τ_i provide an indication of how rapidly BK_i channel availability may be regulated in response to elevations of cytosolic Ca^{2+}. Clearly, an elevation of cytosolic Ca^{2+} into the micromolar range persisting for several hundred milliseconds at potentials of −20 to −50 mV will markedly alter BK_i channel availability. In fact, it has been previously shown that muscarinic acetylcholine receptor activation results in elevations of cytosolic Ca^{2+} to concentrations estimated to be ~1–4 μM (Herrington et al., 1995; Prakriya et al., 1996), which are correlated with inactivation of BK_i current. Thus, the properties of BK channels described here would be consistent with the possibility that a normal receptor-mediated Ca^{2+} elevation in chromaffin cells could dynamically regulate BK channel availability.

Rates of inactivation from closed states are appreciable

For both BK_i and $\alpha + \beta 2$ currents, the maximal peak current activated by depolarizing steps from the most negative holding potentials was consistently smaller at 4 μM than at 60 μM. Part of the difference in peak current might arise from asynchrony of channel activation at the lower Ca^{2+}. However, another factor that might contribute to the apparent reduction in peak current amplitude with 4 μM Ca^{2+} is that, during a depolarizing voltage-step, a significant number of channels may inactivate from closed states prior to ever opening.

To address this issue with macrosopic currents, we have compared the current integral resulting from activation of BK_i channels in chromaffin cell patches when currents are activated at either 4 or 10 μM [Ca^{2+}] at a potential producing near maximal current activation. If channels must open before inactivating, the resulting maximum integrate current level should be identical whether the channels open rapidly or more slowly. This prediction stems from the fact that, in any inactivation model in which channels can only inacti-

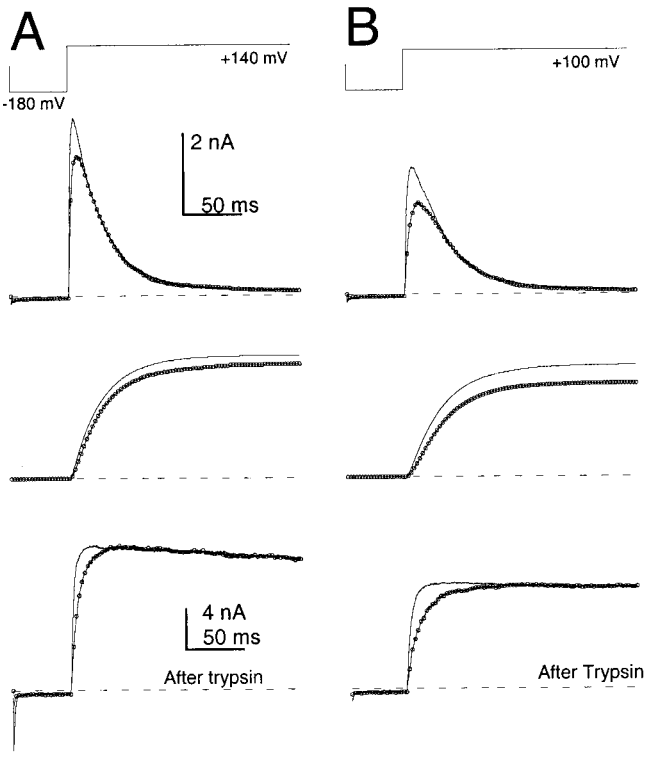

FIGURE 10 With strong depolarizations and 4 μM Ca^{2+}, some channels inactivate without ever opening. (*A*) $\alpha + \beta 2$ currents in an inside-out patch from an oocyte were activated by the indicated voltage protocol at either 10 μM Ca^{2+} or 4 μM (○) Ca^{2+}. Top traces shows actual currents. Middle traces show current integrals, and the bottom traces show currents after brief application of trypsin to remove inactivation. Similarity of maximal current amplitude after trypsin application indicates that these stimulation conditions produce a maximal activation of conductance. Activation time constants after trypsin application were 2.53 and 6.81 ms for 10 and 4 μM Ca^{2+}, respectively. (*B*) Traces show results from the same patch but with a command step to +100 mV. Again, application of trypsin shows the same level of activation of conductance, yet the current integral is markedly reduced in 4 μM Ca^{2+}. Activation time constants were 3.98 and 11.54 for 10 and 4 μM Ca^{2+}, respectively.

vate from open states, the average total amount of time a channel will spend in open states before inactivating will be identical irrespective of how fast the channels activate. In patches from chromaffin cells, the current integral activated at +80 mV with 4 μM Ca^{2+} was about 80% of that observed with 10 μM Ca^{2+} (not shown). This argues that, even under conditions of relatively rapid, near maximal current activation, an appreciable number of channels become inactivated without ever opening. Similar experiments were also done with $\alpha + \beta 2$ currents (Fig. 10 *A*). A conditioning potential of −180 mV was used to remove all channels from resting inactivation. A depolarizing step to +100 mV or +140 mV was used to produce near maximal current activation. To confirm that, at a given voltage step, both 4 and 10 μM Ca^{2+} were sufficient to produce maximal current activation, brief trypsin application was used to remove inactivation, thereby showing that the same maximal peak current was achieved with both [Ca^{2+}] (Fig. 10). Despite the similar peak current activation for both 4 and 10 μM Ca^{2+} at both +100 and +140 mV, the current integral obtained with 4 μM Ca^{2+} was ~10–20% smaller than that with 10 μM Ca^{2+} when the inactivation mechanism is intact. This supports the idea that a substantial fraction of channels may inactivate directly from closed states. For eight patches, at +140 mV, the maximal current integral at 4 μM was 90.1 ± 3.6% of that at 10 μM, whereas, at +100 mV, the maximal current integral at 4 μM was 84.0 ± 3.4% of that at 10 μM. Thus, the slower activation of current at +100 mV apparently results in somewhat more channels inactivating from closed states than from open states than at +140 mV.

A comparison of steady-state inactivation curves in Figs. 1–3 with activation curves (Fig. 1) indicates that many channels may inactivate at potentials over which channel opening is minimal, also suggesting that inactivation from closed states may be appreciable. We therefore examined the extent to which inactivation from closed states may occur at [Ca^{2+}] and voltages where activation of BK_i channels is less favored. To accomplish this, we examined, in patches from chromaffin cells containing from one to three BK_i channels, the ability of a depolarizing conditioning step to produce inactivation, dependent on whether an opening occurs during that conditioning step.

An example of such a patch with 3 BK_i channels is shown in Fig. 11. Channel openings were activated with 10 μM Ca^{2+} by a step to +80 mV following conditioning steps to −140 mV. Following at least 200 ms at −140 mV, the probability that a channel will open during the step to +80 mV is quite high. In contrast, if following removal from inactivation at −140 mV, the patch is stepped to −40 mV for 50 ms, the probability that a channel will open is reduced to less than 50%. If channels are more likely to inactivate from open states than closed states, those traces that exhibit openings during the step to −40 mV should result, on average, in a reduced likelihood of subsequent channel openings during the step to +80 mV, in comparison to traces that do not exhibit openings at −40 mV. Sweeps were therefore separately grouped into those with prepulse openings (Fig. 11 *B*) and those without (Fig. 11 *A*). The resulting averages of peak current activated at +80 mV following the conditioning step are quite similar in the two cases, in fact being somewhat larger when openings are observed during the prepulse to −40 mV. Because the prepulse step to −40 mV does not consistently activate all three channels in the patch, this test does not directly compare the dependence of channel inactivation at +80 mV on whether an opening occurs at −40 mV. However, the result shows clearly that substantial inactivation occurs during the steps to −40 mV even when channel openings are not observed. Furthermore, the results suggest that channels are as likely to inactivate from closed states as from open states.

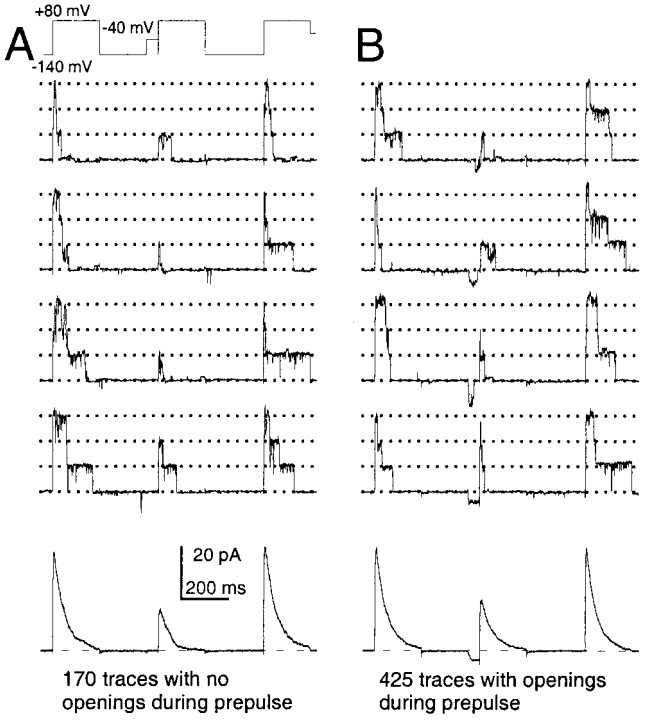

FIGURE 11 At the single-channel level, inactivation of channels occurs in the absence of channel opening. An inside-out patch from a rat chromaffin cell was activated repeatedly with the indicated voltage protocol with 10 μM Ca^{2+} bathing the cytosolic face of the patch. The voltage protocol contains four test periods: P1 is a control step to +80 mV following a step to −140 mV; P2 is a 50-ms step to −40 mV following recovery at −140 mV; P3 is a step to +80 mV following the conditioning step to −40 mV; and P4 is a final test step to +80 mV to show that a recovery step to −140 mV can produce recovery from inactivation. For this patch containing three channels, in almost all cases, periods P1 and P3 result in opening of all three BK channels. (*A*) Selected traces show examples in which no openings were detected during P2. (*B*) Traces show examples in which openings did occur during P2. In this patch, 170 sweeps exhibited no openings during P2, whereas 425 traces had at least one opening during P2. Averages of each of these sets of traces are shown at the bottom, and indicate that, even for traces in which no openings occurred during P2, inactivation is just as likely to occur as in the set of traces in which openings were observed.

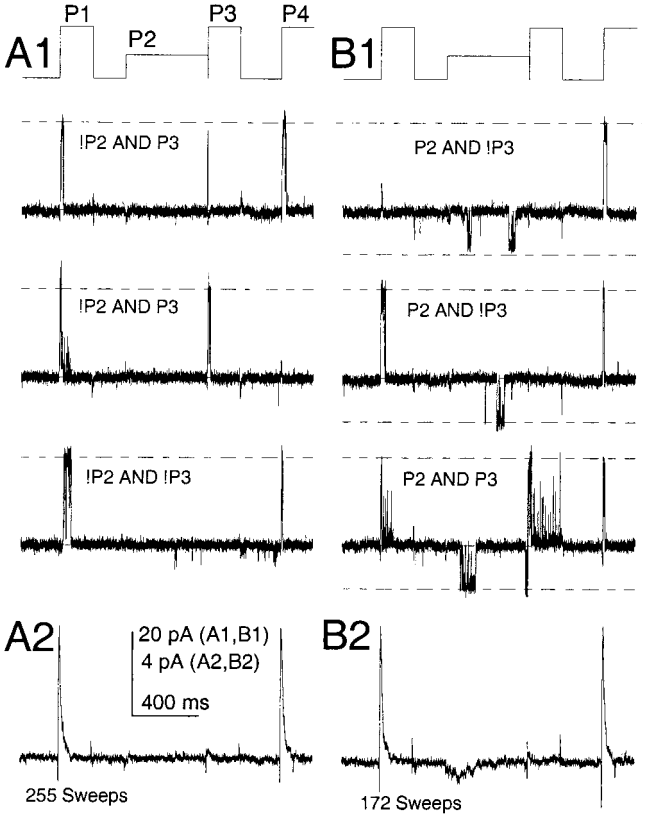

FIGURE 12 Direct evidence that inactivation from closed states of single BK_i channels is appreciable. An inside-out patch from a rat chromaffin cell was bathed with 10 μM Ca^{2+} and stimulated repeatedly with the voltage protocol shown on the top. The presence or absence of channel openings were determined in segments P1, P2, P3, and P4. (*A1*) Sample currents in which no opening was observed during segment P2 (!P2) are shown. In the top two sweeps, a subsequent opening during P3 is observed (!P2 and P3), whereas the third trace shows an example with no opening during P3 (!P2 and !P3). For a total of 427 sweeps, 255 had no opening in P2. Of these, 237 (92.9%) had no opening during P3 (!P2 and !P3). Thus, inactivation has occurred without passage through open states. 18 traces (7.1%) had openings during P3 (!P2 and P3). (*A2*) The average of all traces with no openings during P2 is displayed. (*B1*) traces show sample sweeps of a set of 172 sweeps in which an opening was observed during P2. The top two traces show examples with no opening during P3 (P2 and !P3: 161 of 172 sweeps, 93.6%), whereas the bottom trace shows a case where an opening during P2 is accompanied by an opening during P3 (P2 and P3: 11 of 172, 6.4%). (*B1*) The bottom trace was unusual in that the P3 step occurred during the channel opening in P2. (*B2*) The average current for cases in which an opening was observed occurred during P2 is displayed.

To examine more directly the extent to which inactivation may or may not be coupled to channel opening, we used a similar protocol in single-channel patches from chromaffin cells. Four stimulation protocols were examined: prepulses to −40 mV of either 50 or 500 ms with either 2 or 10 μM Ca^{2+}. Each sweep was considered to consist of four test periods: P1 was the initial test step to +80 mV, P2 was the conditioning step to −40 mV, P3 was the post-conditioning step to +80 mV, and P4 was a final test step to +80 mV following recovery at −140 mV. Openings during P1 and P4 establish the control probability that a channel will open during the test step to +80 mV and also ensure that a channel may not have entered a particularly long-lived inactivated condition, different from the rapid inactivation being examined here. For each sweep, four P2:P3 possibilities exist: closed–closed (!P2, !P3), closed–open (!P2, P3), open–closed (P2, P3), and open–open (P2, P3). We are concerned with two primary questions. First, how likely is it that channel inactivation occurs during P2 without openings in P2? Second, how does the rate of inactivation from closed and open states compare?

Figure 12 shows examples from an experiment with a 500-ms prepulse to −40 mV with 10 μM Ca^{2+}. For this patch, control steps to +80 mV following a prepulse to

−140 mV resulted, on average, in openings in 64.4% of the P1 segments and 64.2% of the P4 segments. These estimates of the fractional availability at −140 mV for this patch are somewhat lower than the 82.0% reported earlier for Fig. 5. When a step to +80 mV is preceded by a 500-ms conditioning step to −40 mV, for the full set of 427 sweeps, only 29 (3.3%) exhibited openings during P3, indicative that, at the end of the step to −40 mV, the channel was very likely to be inactivated. We then divided the set of sweeps into those in which no opening was observed during P2 (Fig. 12 *A*) and those in which an opening was observed during P2 (Fig. 12 *B*). A total of 255 of 427 sweeps exhibited no detectable opening during P2 (Fig. 12 *A*). Yet, 237 of these or 92.9% had no opening during P3, indicative that inactivation at the end of P2 had occurred without channel opening. In comparison, of the 172 sweeps with openings during P2, 161 (93.6%) exhibited no opening during P3, also indicative than inactivation had occurred during P2. The averaged set of traces either without (!P2) or with (P2) an opening during P2 also show that inactivation proceeds just as effectively at −40 mV and 10 μM whether an opening occurs or not.

It could be suggested that, because inactivation is virtually complete by 500 ms, perhaps inactivation from open states is actually much more likely, but that the 500-ms duration of the P2 step allows the more rare inactivation from closed states to be observed. However, even with 50-ms steps to −40 mV, a similar fractional reduction in channel availability is seen whether or not an opening is observed during the P2 step. This is displayed graphically in Fig. 13, in which the probability of observing an opening during P3 is plotted as a duration of the conditioning step. For all sweeps, the reduction in that probability is similar to the time course of inactivation given for 10 μM Ca^{2+} at −40 mV in Fig. 9. However, when the probability of opening during P3 is determined separately for sweeps in which a P2 opening is or is not observed, a similar time course of inactivation onset is obtained. Thus, the occurrence of channel opening during P2 does not increase the likelihood that the channel will be in the inactivated condition at the end of P2.

Table 1 summarizes the results for several patches. Although the results do not allow explicit estimation of the rates of onset of inactivation from closed states and open states, it is clear that channels can directly inactivate without ever passing through open states. Table 1 also provides the probabilities of !P3 conditional on whether an opening occurred in P2. These values also support the view that channel inactivation is quite likely, irrespective of whether channel opening occurs at −40 mV. In fact, there is essentially no indication that an opening during P2 increases the likelihood that the channel will be inactivated at the end of P2. Thus, opening during P2 does not appear to be increasing the rate of channel inactivation during P2.

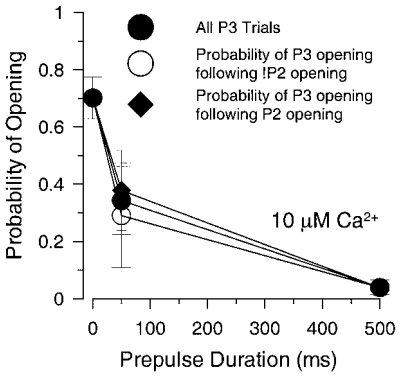

FIGURE 13 The rate of inactivation is similar whether channel opening occurs or not. The probability that channel opening would occur during a step to +80 mV with 10 μM Ca^{2+} was plotted as a function of the duration of a conditioning step to −40 mV. The values at the 0 time point correspond to the control probability of a channel opening occurring during P1 and P4 steps. Following conditioning steps of either 50 or 500 ms, the probability that an opening would occur was determined separately for all P3 steps to +80 mV (●), for P3 steps contingent on no openings during P2 (○), and for P3 steps contingent on an opening occurring during P2 (◆). Some of the excess of openings seen in P3, when an opening does occur in P2 may arise from channels being open at the end of P2. Points correspond to the mean and SDs of four patches at 50 ms, and three patches at 500 ms. Direct calculation of the event probabilities by lumping sweeps from all patches yielded similar results.

DISCUSSION

Inactivation of BK_i channels in rat chromaffin cells shares features with rapid inactivation of other voltage-dependent channels. It involves multiple, trypsin-sensitive cytosolic residues (Solaro and Lingle, 1992; Solaro et al., 1995; Ding et al., 1998). The apparent rate of inactivation is increased by depolarization or increases in cytosolic [Ca^{2+}] that increase the rate at which channels open (Solaro and Lingle, 1992). However, the inactivation rate reaches a limiting value once the activation rate appears to exceed the intrinsic inactivation rate. Thus, it has been proposed that the voltage- and Ca^{2+}-dependence of inactivation of BK_i channels arises from coupling of a relatively voltage-independent and Ca^{2+}-independent inactivation to activation steps that are voltage- and Ca^{2+}-dependent. Here we have examined the properties of BK_i channel availability as a function of voltage and Ca^{2+}, the properties of inactivation onset at moderate activation voltages and Ca^{2+}, and the ability of closed channels to undergo inactivation. Some aspects of BK_i function were also directly compared to properties of heterologously expressed $\alpha + \beta 2$ currents, to ascertain to what extent the properties of these subunits may mirror native BK_i currents.

The primary conclusions concerning mechanistic details of inactivation of native BK_i channels are the following. First, there is no strictly Ca^{2+}-dependent inactivation up to 60 μM Ca^{2+}; second, voltage-dependent transitions are sufficient to produce inactivation in the absence of Ca^{2+};

TABLE 1 Event probabilities under various conditions

	50 ms, 2 μM		500 ms, 2 μM		50 ms, 10 μM		500 ms, 10 μM	
Dependencies*	$N^{\dagger}$	Fraction‡	$N^{\dagger}$	Fraction‡	$N^{\dagger}$	Fraction‡	$N^{\dagger}$	Fraction‡
Total sweeps	867	(4 patches)	447	(3 patches)	604	(4 patches)	804	(3 patches)
P2 and !P3	7	0.008	4	0.009	118	0.195	355	0.442
!P2 and P3	517	0.596	298	0.667	148	0.245	22	0.027
P2 and P3	6	0.007	10	0.022	69	0.114	16	0.020
!P2 and !P3	337	0.389	135	0.302	269	0.445	411	0.511
P2	13	0.015	14	0.031	187	0.309	371	0.461
P3	523	0.603	308	0.689	217	0.359	38	0.047
P1	646	0.745	359	0.803	418	0.692	553	0.688
P4	635	0.732	365	0.817	402	0.666	556	0.692
!P3 given P2	0.538	(7/13)	0.286	(4/14)	0.631	(118/187)	0.957	(355/371)
!P3 given !P2	0.395	(337/854)	0.312	(135/433)	0.645	(269/417)	0.949	(411/433)

*P1 to P4, segments of the stimulation protocol given in Fig. 12, during which the probability of occurrence of a channel opening in a single channel patch was determined; P2 and !P3, occurrences of an opening in P2 with no opening in P3; and so on. P1, P3, and P4 were steps to +80 mV, whereas P2 was a step to −40 mV. Prior to P1 and P4, the potential was stepped to −140 mV for 240 ms, whereas, prior to P2, the potential was stepped to −140 mV for either 200 or 240 ms.

$^{\dagger}N$, the number of times a particular event was observed out of the total number sweeps.

‡Fraction, the ratio of N to the total sweeps.

third, there is appreciable inactivation from closed states, and a key conformational change required to permit inactivation likely occurs prior to channel opening. In addition, both the onset of inactivation and steady-state properties of inactivation suggest that substantial regulation of BK_i channel availability may occur at relatively negative holding potentials. All the mechanistic features of the BK_i currents described above were also shown to apply, in general, for currents arising from heterologously expressed $\alpha + \beta 2$ currents, supporting the view that these subunits probably participate, at least in part, in the formation of BK_i channels.

Comparison of native BK_i channels and $\alpha + \beta 2$ currents

Qualitatively, native BK_i channels and $\alpha + \beta 2$ currents share many properties. The voltage- and Ca^{2+}-dependence of inactivation onset appears similar. The voltages of half availability at a given $[Ca^{2+}]$ are comparable. Coupled with the presence of message for the $\beta 2$ subunit in rat chromaffin cells (Xia et al., 2000), it seems quite likely that the $\beta 2$ subunit is an important molecular determinant of the inactivation behavior in rat chromaffin cells. However, native BK_i currents appear to differ from $\alpha + \beta 2$ currents in several ways. First, the voltage dependence of activation at at given $[Ca^{2+}]$ (Prakriya et al., 1996) is somewhat right-shifted in comparison to that arising from $\alpha + \beta 2$ currents (Wallner et al., 1999; Xia et al., 1999). Similarly, as shown here, the voltage dependence of steady-state inactivation for BK_i currents is somewhat right-shifted in comparison to $\alpha + \beta 2$ currents. These shifts are not large, being at most 20–30 mV.

The shifts in $V_{0.5}$ for either activation or inactivation might be expected if, in native chromaffin cells, BK_i channels contained less than a full complement of four $\beta 2$ subunits. A proposal of this sort has been previously made to account for variability in inactivation properties of BK_i currents among different chromaffin cells (Ding et al., 1998). However, it remains unknown whether the proposed variability in average number of $\beta 2$ subunits per channel in chromaffin cells may arise simply by expression of fewer $\beta 2$ subunits or by titration with a second type of β subunit. Northern blots of human adrenal medullae do indicate the presence both of some form of $\beta 3$ subunit (Xia et al., 2000) and also the $\beta 4$ subunit (X.-M. Xia and C. J. Lingle, unpublished observations). $\beta 3$ splice variants exhibit several different behaviors including noninactivating ($\beta 3$d), and inactivating ($\beta 3$a–c) forms with both the $\beta 3$a variant (~35 ms) and the $\beta 3$c variant (~50 ms) exhibiting time constants of inactivation not much different from that of the $\beta 2$ variant (Uebele et al., 2000). Because the $\beta 3$ variants do not produce an intrinsic shift in the $V_{0.5}$ for activation at a given $[Ca^{2+}]$ (Brenner et al., 2000; Zeng et al., 2001), it might be possible to explain some features of chromaffin-cell BK_i currents from mixtures of $\beta 2$ and $\beta 3$ subunits. Some properties of the $\beta 3$a and $\beta 3$c variants will be presented in a subsequent paper (J. P. Ding and C. J. Lingle, in preparation).

There is no intrinsic Ca^{2+} dependence of inactivation, but voltage-dependent transitions are sufficient to allow maximal rates of inactivation

Evaluation of the steady-state inactivation properties of BK_i (and $\alpha + \beta 2$) currents indicates that 50% channel availability is shifted to more negative voltages with elevations in cytosolic $[Ca^{2+}]$ up through 60 μM. We find no evidence

that the dependence of steady-state inactivation on $[Ca^{2+}]$ begins to saturate up through 60 μM. Whereas the steady-state availability of voltage-dependent ion channels is defined by a single voltage of half availability, for BK_i channels half availability is both Ca^{2+}- and voltage-dependent. Because of the participation of both Ca^{2+}- and voltage-dependent transitions in the activation of the BK channels, the dependence of channel availability on both $[Ca^{2+}]$ and voltage presumably arises from the coupling of inactivation to activation. If Ca^{2+}-dependent transitions were sufficient to lead to channel states that were permissive for inactivation, at sufficiently negative potentials, robust elevations of $[Ca^{2+}]$ might be expected to reveal such strictly Ca^{2+}-dependent inactivation. However, single-channel experiments presented here indicated that, at 10 μM Ca^{2+}, the maximal fractional availability of any individual channel exceeds 0.85 at sufficiently negative potentials. Furthermore, if $[Ca^{2+}]$ is elevated to 60 μM, a similar maximal fractional availability is reached at negative potentials. Thus, taking into account long-lived closed states that are observed, it appears that, at negative potentials, all BK_i channels may be available for activation at either 10 or 60 μM. Thus, at least through 60 μM Ca^{2+}, Ca^{2+} alone is not sufficient to drive the channels into states that can then inactivate.

In contrast, in the virtual absence of Ca^{2+}, depolarizations to +40 mV and more positive produce inactivation of BK_i channels (and $\alpha + \beta 2$ channels). Furthermore, at sufficiently positive potentials, macroscopic inactivation of BK_i and $\alpha + \beta 2$ channels approaches the same limiting values observed with higher Ca^{2+}. Thus, voltage-dependent transitions, in the complete absence of Ca^{2+}, are sufficient to allow inactivation to occur, whereas the intrinsic rate of channel inactivation appears to be defined by voltage-independent transitions.

The shift in steady-state inactivation with $[Ca^{2+}]$ arises naturally from the coupling of inactivation to activation. This phenomenon provides the mechanistic basis by which BK_i channel availability may be regulated by modest elevations of cytosolic $[Ca^{2+}]$ (Herrington et al., 1995).

Closed-state inactivation

Several aspects of our results indicate that inactivation from closed states of BK_i and $\alpha + \beta 2$ currents is appreciable. This was shown most directly in single-channel experiments in which the onset of inactivation at 10 μM Ca^{2+} and −40 mV occurs with a similar time course, whether the channel has opened or not. The macroscopic current experiments comparing current integrals would also suggest that inactivation from some closed states must also be rather rapid, because, in these experiments, channel opening occurs fairly rapidly. For example, the difference between the current integrals activated with 4 and 10 μM Ca^{2+} was observed both at +100 and +140 mV (Fig. 10). Once open, it takes on average about 20 ms for a channel to inactivate at these voltages. In contrast, the activation time constants at +140 mV for 10 and 4 μM Ca^{2+} were ~2.5 and 6.8 ms, respectively, and, at +100 mV, ~3.9 and 11.5 ms, respectively. These values are similar to those reported for $\alpha + \beta 2$ currents for a $\beta 2$ construct with the N-terminus removed (Brenner et al., 2000). Thus, it takes a channel, on average, 2–3 times longer until it first opens at 4 μM than at 10 μM. Yet, this delay until opening is still relatively brief, in comparison to the average of ~20 ms it takes an open channel to inactivate. Thus, each channel, on average, spends very little time in closed states, prior to opening. To account for the observed reduction in current integral at 4 μM Ca^{2+}, inactivation rates from closed states must be fairly rapid. Because there is essentially no appreciable resting inactivation prior to the voltage steps and the intrinsic rates of inactivation themselves appear to be voltage independent, we infer that voltage-dependent transitions result in some closed state from which inactivation is likely. If inactivation from closed states can occur so readily, why does the macroscopic τ_i exhibit a dependence on voltage and Ca^{2+} (Solaro and Lingle, 1992; Xia et al., 1999)? This would arise from the fact that inactivation does not occur from closed states per se, but from a particular set of closed states that is only entered with some delay following depolarization. Although Ca^{2+} itself is apparently insufficient to cause entry into inactivation permissive states, binding of Ca^{2+} may allosterically act to enhance rates of voltage-dependent transitions that lead to inactivation.

Inactivation from closed states has been observed for a number of voltage-gated channels (Aldrich et al., 1983; Aldrich and Stevens, 1987; Jerng et al., 1999). However, for the *Shaker*B K^+ channel, the idea that opening is a prerequisite for inactivation is well established (Zhou et al., 2001). This idea that opening is required for inactivation is also coupled with the idea that, for a channel to return to a closed conformation, the inactivation domain must first dissociate from its binding site (Demo and Yellen, 1992; Ruppersberg et al., 1991; Kuo, 1997). In contrast, BK_i and $\alpha + \beta 2$ channels return to resting states without ever passing through open states (Solaro et al., 1997; for $\alpha + \beta 2$ channels; C. J. Lingle, unpublished observations). Thus, this latter observation would suggest that occupancy by the BK inactivation domain of its binding site does not hinder any open-to-closed conformational change. Together, these results would suggest that the binding site is revealed not by channel opening, but by a conformational change that precedes channel opening. It remains to be seen how the structural details of BK channel inactivation can be reconciled with structural information available from *Shaker* (Zhou et al., 2001).

Models of BK gating and inactivation

Although it is beyond the scope of the present paper to test a model for BK gating and inactivation, it is useful to define the minimal properties of a scheme that we feel accounts for the various observations that have been made concerning BK activation and inactivation. The key points that must be explained are that: Ca^{2+}-dependent transitions alone do not result in inactivation, voltage-dependent transitions are sufficient to allow inactivation, and inactivation may occur as readily from some particular closed state as from open states. A model that contains these essential features and also incorporates the idea that each subunit in the BK channel tetramer may bind a Ca^{2+} ion (Cox et al., 1997) is given as

$$\begin{array}{ccc} C1_m & & \\ \uparrow\downarrow L1(V) & & \\ C2_m & \rightleftharpoons & I2_m \\ \uparrow\downarrow L2(V) & & \uparrow\downarrow \\ O_m & \rightleftharpoons & I3_m \end{array}$$

SCHEME 1

where $C1_m$ corresponds to

$$C1_0 \overset{4K_c}{\rightleftharpoons} C1_1 \overset{3K_c/2}{\rightleftharpoons} C1_2 \overset{2K_c/3}{\rightleftharpoons} C1_3 \overset{K_c/4}{\rightleftharpoons} C1_4,$$

indicative that any given state may have 0–4 Ca^{2+} ions bound, and L1(V) and L2(V) represent two distinct voltage-dependent transitions leading to channel opening. Such a model is a simple extension of the 10-state Monod–Wyman–Changeux model originally evaluated for *Slo1* currents by Cox and Aldrich (1997), with the inclusion of an additional layer of closed states ($C2_m$). The possibility of an additional layer of closed states and two separate voltage-dependent transitions leading to channel opening has been previously suggested in other work (Rothberg and Magleby, 2000; Zeng et al., 2001). A limitation of Scheme 1 is that it does not incorporate the idea that the independent movement of four voltage-sensors, one per subunit, is an essential element of the gating process.

Although Scheme I may contain the general features required by our data, more recent models of the voltage and Ca^{2+} dependence of BK activation utilize a two-tiered 50-state model that assumes the independent binding of four Ca^{2+} ions and the movement of four voltage sensors (Rothberg and Magleby, 1999, 2000; Cox and Aldrich, 2000). Such a model, given in abbreviated form in Scheme 2, arises naturally from the tetrameric nature of the channel and the idea that each subunit contains a binding site for Ca^{2+} and a voltage-sensor.

$$C_{m,n} \overset{L(V)}{\rightleftharpoons} O_{m,n}$$

SCHEME 2

where $C1_{m,n}$ and $O_{m,n}$ each correspond to a tier of 25 states, reflecting the binding of $m = 0, 4$ Ca^{2+} ions and the movement of $n = 0, 4$ voltage sensors, with L(V) reflecting the equilibrium between closed and open states. It is possible to incorporate the general properties of inactivation we have observed into this model by proposing that voltage-sensor movement is directly associated with the critical conformational change necessary to allow inactivation to occur. Such a conformational change would precede channel opening. Furthermore, Ca^{2+}-dependent transitions would not directly lead to inactivation, but would facilitate inactivation resulting from voltage-dependent transitions.

Finally, we consider one other scheme that arises from recent results suggesting an extension of Scheme 2. Namely, our previous work with $\alpha + \beta 3b$ currents has suggested that an additional tier of closed states may also precede channel opening (Zeng et al., 2001), and this has also been suggested by others (Rothberg and Magleby, 2000). The most general formulation of this sort of model including inactivation steps is given in

$$\begin{array}{ccccc} C1_{m,n} & \overset{k_f}{\underset{k_r}{\rightleftharpoons}} & C1^*_{m,n} & \overset{k_b}{\underset{k_u}{\rightleftharpoons}} & I1_{m,n} \\ \uparrow\downarrow L1(V) & & \uparrow\downarrow & & \uparrow\downarrow \\ C2_{m,n} & \rightleftharpoons & C2^*_{m,n} & \rightleftharpoons & I2_{m,n} \\ \uparrow\downarrow L2(V) & & \uparrow\downarrow & & \uparrow\downarrow \\ O_{m,n} & \rightleftharpoons & O^*_{m,n} & \rightleftharpoons & I3_{m,n} \end{array}$$

SCHEME 3

This model also includes steps to take into account the two-step inactivation mechanism proposed to occur with β subunits of BK channels (Lingle et al., 2001). As in Scheme 2, for each element in Scheme 3, $m = 0–4$ corresponds to the number of Ca^{2+} ions bound, and $n = 0–4$ to the number of voltage-sensors in an active position. Thus, each element (e.g., $C1_{m,n}$, $C2_{m,n}$, etc.) corresponds to a separate 25-state tier given in earlier models of BK channel activation (Cox and Aldrich, 2000; Rothberg and Magleby, 1999, 2000), where each subunit in the BK channel tetramer contains a Ca^{2+} binding site and a voltage sensor. States C1*, C2*, and O* correspond to preinactivated states reflecting the two-step inactivation mechanism (Lingle et al., 2001). Here, for Scheme 3, L1(V) corresponds to a weakly voltage-dependence conformational change in the closed channel, separate from voltage-sensor movement, that precedes the also weakly voltage-dependent opening of the channel, L2(V). This additional tier of closed states would therefore reflect a conformational change in the closed channel that is

allosterically regulated by Ca^{2+} and voltage. L1(V) would therefore represent the critical conformational change that is required for inactivation to proceed. Because the transition defined by L1(V) is allosterically regulated by both Ca^{2+} and voltage, one might expect that Ca^{2+} itself would be able to produce inactivation even at negative potentials. However, as long as Ca^{2+}-dependent transitions do not lead directly to opening, any model in which there is intrinsic voltage dependence in the final steps to channel opening will predict that inactivation will never result strictly from Ca^{2+} alone. Because of the intrinsic voltage dependence of L1, Ca^{2+} alone will be insufficient to produce inactivation.

We have now proposed two general sorts of physical models that might account for the properties of inactivation we have observed. In one case, inactivation is proposed to result from a conformational change specifically associated with voltage-sensor movement. In the other, a conformational change within the closed channel, allosterically regulated by Ca^{2+} and voltage, is the essential step required for inactivation. Future work will be required to evaluate whether either sort of physical mechanism provides a better account of BK channel inactivation.

This work was supported by DK-46564 and NS-37671 from the National Institutes of Health.

REFERENCES

Adelman, J. P., K. Z. Shen, M. P. Kavanaugh, R. A. Warren, Y. N. Wu, A. Lagrutta, C. T. Bond, and R. A. North. 1992. Calcium-activated potassium channels expressed from cloned complementary DNAs. *Neuron.* 9:209–216.

Aldrich, R. W., D. P. Corey, and C. F. Stevens. 1983. A reinterpretation of mammalian sodium channel gating based on single channel recording. *Nature.* 306:436–441.

Aldrich, R. W., and C. F. Stevens. 1987. Voltage-dependent gating of single sodium channels from mammalian neuroblastoma cells. *J. Neurosci.* 7:418–431.

Brenner, R., T. J. Jegla, A. Wickenden, Y. Liu, and R. W. Aldrich. 2000. Cloning and functional characterization of novel large conductance calcium-activated potassium channel beta subunits, hKCNMB3 and hKCNMB4. *J. Biol. Chem.* 275:6453–6461.

Butler, A., S. Tsunoda, D. P. McCobb, A. Wei, and L. Salkoff. 1993. mSlo, A complex mouse gene encoding "maxi" calcium-activated potassium channels. *Science.* 261:221–224.

Cannell, M. B., and C. G. Nichols. 1991. Effects of pipette geometry on the time course of solution change in patch clamp experiments. *Biophys. J.* 60:1156–1163.

Cox, D., and R. Aldrich. 2000. Role of the β1 subunit in large-conductance Ca^{2+}-activated K^+ channel gating energetics. Mechanisms of enhanced Ca^{2+} sensitivity. *J. Gen. Physiol.* 116:411–432.

Cox, D. H., J. Cui, and R. W. Aldrich. 1997. Allosteric gating of a large conductance Ca-activated K^+ channel. *J. Gen. Physiol.* 110:257–281.

Cui, J., and R. W. Aldrich. 2000. Allosteric linkage between voltage and Ca^{2+}-dependent activation of BK-type mslo1 K^+ channels. *Biochemistry.* 39:15612–15619.

Demo, S. D., and G. Yellen. 1992. Ion effects on gating of the Ca^{2+}-activated K^+ channel correlate with occupancy of the pore. *Biophys. J.* 61:639–648.

Ding, J. P., Z. W. Li, and C. J. Lingle. 1998. Inactivating BK channels in rat chromaffin cells may arise from heteromultimeric assembly of distinct inactivation-competent and noninactivating subunits. *Biophys. J.* 74:268–289.

Fenwick, E. M., A. Marty, and E. Neher. 1982. Sodium and calcium channels in bovine chromaffin cells. *J. Physiol. (Lond.).* 331:599–635.

Hamill, O. P., A. Marty, E. Neher, B. Sakmann, and F. J. Sigworth. 1981. Improved patch-clamp techniques for high-resolution current recording from cells and cell-free membrane patches. *Pflugers Arch.* 391:85–100.

Herrington, J., C. R. Solaro, A. Neely, and C. J. Lingle. 1995. The suppression of Ca^{2+}- and voltage-dependent outward K^+ current during mAChR activation in rat adrenal chromaffin cells. *J. Physiol. (Lond.).* 485:297–318.

Horrigan, F. T., and R. W. Aldrich. 1999. Allosteric voltage gating of potassium channels II. Mslo channel gating charge movement in the absence of Ca^{2+}. *J. Gen. Physiol.* 114:305–336.

Horrigan, F. T., J. Cui, and R. W. Aldrich. 1999. Allosteric voltage gating of potassium channels I. Mslo ionic currents in the absence of Ca^{2+}. *J. Gen. Physiol.* 114:277–304.

Jerng, H. H., M. Shahidullah, and M. Covarrubias. 1999. Inactivation gating of Kv4 potassium channels: molecular interactions involving the inner vestibule of the pore. *J. Gen. Physiol.* 113:641–660.

Kilpatrick, D. L., R. V. Lewis, S. Stein, and S. Udenfriend. 1980. Release of enkephalins and enkephalin-containing polypeptides from perfused beef adrenal glands. *Proc. Natl. Acad. Sci. U.S.A.* 77:7473–7475.

Kuo, C. C. 1997. Deactivation retards recovery from inactivation in *Shaker* K^+ channels. *J. Neurosci.* 17:3436–3444.

Li, Z. W., J. P. Ding, V. Kalyanaraman, and C. J. Lingle. 1999. RINm5f cells express inactivating BK channels whereas HIT cells express noninactivating BK channels. *J. Neurophysiol.* 81:611–624.

Lingle, C., X.-H. Zeng, J.-P. Ding, and X.-M. Xia. 2001. Inactivation of BK channels mediated by the N-terminus of the β3b auxiliary subunit involves a two-step mechanism: possible separation of binding and blockade. *J. Gen. Physiol.* 117:583–605.

Lingle, C. J., C. R. Solaro, M. Prakriya, and J. P. Ding. 1996. Calcium-activated potassium channels in adrenal chromaffin cells. *Ion Channels.* 4:261–301.

Livett, B. G. 1984. Adrenal medullary chromaffin cells in vitro. *Physiol. Rev.* 64:1103–1161.

Markwardt, F., and G. Isenberg. 1992. Gating of maxi K^+ channels studied by Ca^{2+} concentration jumps in excised inside-out multi-channel patches (myocytes from guinea pig urinary bladder). *J. Gen. Physiol.* 99:841–862.

Neely, A., and C. J. Lingle. 1992. Two components of calcium-activated potassium current in rat adrenal chromaffin cells. *J. Physiol.* 453: 97–131.

Piskorowski, R., and R. Aldrich. 2001. Altering the gating of large-conductance Ca^{2+}-activated K^+ channels with different permeant ions. *Biophys. J.* 80:221a. (Abstract)

Prakriya, M., C. R. Solaro, and C. J. Lingle. 1996. $[Ca^{2+}]_i$ elevations detected by BK channels during Ca^{2+} influx and muscarine-mediated release of Ca^{2+} from intracellular stores in rat chromaffin cells. *J. Neurosci.* 16:4344–4359.

Role, L., and R. Perlman. 1980. Purification of adrenal medullary chromaffin cells by density gradient centrifugation. *J. Neurosci. Methods.* 2:253–265.

Rothberg, B. S., and K. L. Magleby. 1999. Gating kinetics of single large-conductance Ca^{2+}-activated K^+ channels in high Ca^{2+} suggest a two-tiered allosteric gating mechanism. *J. Gen. Physiol.* 114:93–124.

Rothberg, B. S., and K. L. Magleby. 2000. Voltage and Ca^{2+} activation of single large-conductance Ca^{2+}-activated K^+ channels described by a two-tiered allosteric gating mechanism. *J. Gen. Physiol.* 116:75–99.

Ruppersberg, J. P., R. Frank, O. Pongs, and M. Stocker. 1991. Cloned neuronal IK(A) channels reopen during recovery from inactivation. *Nature.* 353:657–660.

Solaro, C. R., J. P. Ding, Z. W. Li, and C. J. Lingle. 1997. The cytosolic inactivation domains of BK_i channels in rat chromaffin cells do not behave like simple, open-channel blockers. *Biophys. J.* 73:819–830.

Solaro, C. R., and C. J. Lingle. 1992. Trypsin-sensitive, rapid inactivation of a calcium-activated potassium channel. *Science.* 257:1694–1698.

Solaro, C. R., M. Prakriya, J. P. Ding, and C. J. Lingle. 1995. Inactivating and noninactivating Ca^{2+}- and voltage-dependent K^+ current in rat adrenal chromaffin cells. *J. Neurosci.* 15:6110–6123.

Uebele, V. N., A. Lagrutta, T. Wade, D. J. Figueroa, Y. Liu, E. McKenna, C. P. Austin, P. B. Bennett, and R. Swanson. 2000. Cloning and functional expression of two families of beta-subunits of the large conductance calcium-activated K^+ channel. *J. Biol. Chem.* 275: 23211–23218.

Wallner, M., P. Meera, and L. Toro. 1999. Molecular basis of fast inactivation in voltage and Ca^{2+}-activated K^+ channels: a transmembrane beta-subunit homolog. *Proc. Natl. Acad. Sci. U.S.A.* 96:4137–4142.

Wei, A., C. Solaro, C. Lingle, and L. Salkoff. 1994. Calcium sensitivity of BK-type KCa channels determined by a separable domain. *Neuron.* 13:671–681.

Xia, X. M., J. P. Ding, and C. J. Lingle. 1999. Molecular basis for the inactivation of Ca^{2+}- and voltage-dependent BK channels in adrenal chromaffin cells and rat insulinoma tumor cells. *J. Neurosci.* 19: 5255–5264.

Xia, X.-M., J. Ding, X.-H. Zeng, K.-L. Duan, and C. Lingle. 2000. Rectification and rapid activation at low Ca^{2+} of Ca^{2+}-activated, voltage-dependent BK currents: consequences of rapid inactivation by a novel β subunit. *J. Neurosci.* 20:4890–4903.

Zeng, X.-H., X.-M. Xia, and C. J. Lingle. 2001. Gating properties conferred on BK channels by the β3b auxiliary subunit in the absence of its N- and C-termini. *J. Gen. Physiol.* 117:607–627.

Zhou, M., J. H. Morais-Cabral, S. Mann, and R. MacKinnon. 2001. Potassium channel receptor site for the inactivation gate and quaternary amine inhibitors. *Nature.* 411:657–661.